Steel and Composite Structures, *Vol. 27, No. 6 (2018) 727-745*
DOI: https://doi.org/10.12989/scs.2018.27.6.727

Finite element simulations on the ultimate response of extended stiffened end-plate joints

Roberto Tartaglia [a], Mario D'Aniello [*], Mariana Zimbru [b] and Raffaele Landolfo [c]

Department of Structures for Engineering and Architecture, University of Naples "Federico II", Via Forno Vecchio 36, 80134 Naples, Italy

(*Received October 8, 2017, Revised March 13, 2018, Accepted April 4, 2018*)

Abstract. The design criteria and the corresponding performance levels characterize the response of extended stiffened end-plate beam-to-column joints. In order to guarantee a ductile behavior, hierarchy criteria should be adopted to enforce the plastic deformations in the ductile components of the joint. However, the effectiveness of thesecriteria can be impaired if the actual resistance of the end-plate material largely differs from the design value due to the potential activation of brittle failure modes of the bolt rows (e.g., occurrence of failure mode 3 in the place of mode 1 per bolt row). Also the number and the position of bolt rows directly affect the joint response. The presence of a bolt row in the center of the connection does not improve the strength of the joint under both gravity, wind and seismic loading, but it can modify the damage pattern of ductile connections, reducing the gap opening between the end-plate and the column face. On the other hand, the presence of a central bolt row can influence the capacity of the joint to resist the catenary actions developing under a column loss scenario, thus improving the joint robustness. Aiming at investigating the influence of these features on both the cyclic behavior and the response under column loss, a wide range of finite element analyses (FEAs) were performed and the main results are described and discussed in this paper.

Keywords: steel bolted joints; seismic design; column loss; robustness; moment-rotation response; cyclic behavior

1. Introduction

Bolted beam-to-column joints are commonly used in steel multi-storey frames and various typologies have been thoroughly investigated in literature (Murray 1990, Leon 1995, Faella *et al*. 2000, Sumner and Murray 2000, 2002, Da Silva *et al*. 2002, Girao Coelho *et al*. 2004, Murray and Sumner 2004, Maggi *et al*. 2005, Guo *et al*. 2006, Shi *et al*. 2007a, b, Iannone *et al*. 2010, Latour *et al*. 2011, 2014, Latour and Rizzano 2013, Abidelah *et al*. 2012, Latour *et al*. 2014, Brunesi *et al*. 2014, 2015, Augusto *et al*. 2016, 2017, Cassiano *et al*. 2018, D'Aniello *et al*. 2018, D'Antimo *et al*. 2018, Latour *et al*. 2018). Among the large number of possible configurations, extended stiffened end-plate bolted (ESEPB) beam-to-column joints are a very popular choice for steel moment resisting frames (MRFs) designed to resist lateral forces (i.e., earthquake and/or wind), thanks to their relatively low constructional costs and the structural effectiveness largely demonstrated by both experimental and analytical studies since the '90s (Murray 1990, Sumner and Murray 2000, 2002 Murray and Sumner 2004, Guo *et al*. 2006, Shi *et al*. 2007a, b, Abidelah *et al*. 2012) Nowadays, ESEPB joints are seismically pre-qualified in the United States of America (USA) within the AISC 358-16 (2016), whose bases were set by Murray and Sumner (2004) that proposed a design method to calculate the strength of end-plate connections on the basis of the theory of yield lines. This methodology was supported by the studies formerly carried out by Sumner and Murray (2000, 2002), which demonstrated that ESEPB joints can provide large energy dissipation capacity with stable hysteretic behavior up to 4% of chord rotation.

In China, the influence of the end-plate thickness was experimentally investigated by Guo *et al*. (2006), which highlighted that the thinner the end-plate the more ductile is the joint response, provided that the design resistance is guaranteed. In addition, these tests showed that stiffened end-plate joints can be more ductile than corresponding unstiffened joints even in the case of partial strength connections due to more favorable damage pattern guaranteed by the presence of rib stiffeners. Shi *et al*. (2007a, b) also carried out both monotonic and cyclic tests in order to investigate the seismic behavior of ESEPB joints and to validate an analytical method to predict the joint response. In particular, these studies highlighted the key role of the rib stiffeners, concluding that extended end-plate connections with rib stiffeners can provide better rotational capacity, ductility and larger stiffness than the unstiffened joints, provided that rational design criteria are used. Abidelah *et al*. (2012) carried out experimental and numerical studies in order to investigate the influence of the rib stiffeners on bolted end-plate joints. In particular, they demonstrated that the ribs modify the position of the center of compression increasing the resisting lever arm of the bolted connection. In Europe, the current version of the

*Corresponding author, Ph.D., Assistant Professor, E-mail: mdaniel@unina.it
[a] Ph.D.
[b] Ph.D. Student
[c] Ph.D., Professor

http://www.techno-press.org/?journal=scs&subpage=6 ISSN: 1229-9367 (Print), 1598-6233 (Online)

Eurocodes (i.e., EN1993:1-8 and EN1998-1) does not provide neither specific requirements nor codified prequalification procedures for seismic resistant extended stiffened end-plate joints. However, a prequalification procedure and the design criteria for seismic resistant ESEPB joints have been recently developed within the framework of the EQUALJOINTs research project (RFSR-CT-2013-00021). It is also worth noting that the performance criteria presented by D'Aniello *et al*. (2017b) are currently implemented in the 2nd draft (v.2.1) of the amended EN 1993-1-8, currently under the revision of the CEN/TC 250/SC 3 experts.

According to D'Aniello *et al*. (2017b), the design objectives can be achieved by imposing the hierarchy of resistances between the beam, the connection and the column web panel in order to avoid any brittle failure mode. In this framework, a key parameter affecting the joint behavior is the strength of the end-plate (EP), which can impair the effectiveness of the hierarchy of resistances among the main components of the joint. The strength of the end-plate is directly dependent on the yield stress of the steel and the arrangement of bolts.

With this regard, it is well known that the variability of the yield stress of steel plates produced in European market is relatively high (Piluso and Rizzano 2007, Piluso *et al*. 2012, Latour and Rizzano 2013), due to both the variability of the chemical composition (as shown by OPUS and SAFEBRICTILE research projects) and finishing processes for the rectification of plate (OPTIFIN research project). In addition, in the experience of the Authors, it is quite common in the constructional practice that the actual mechanical features of the plates provided by the supplier can be either non-compliant with the design requirements or non-conforming to the material certificate (being the traceability of the steel material still an unsolved issue in some countries of Southern Europe, like Italy). These circumstances can be highly non-conservative because the use of an end-plate with steel strength different from the design value, can substantially affect the joint resistance, the ductility and the corresponding failure mode.

Indeed, even though the strength of the connection can increase with the steel yield stress, premature and undesired failure of bolts (i.e., mode 3) with very poor associated rotational capacity, can be activated in partial strength connections. On the contrary, end-plate yield strength significantly smaller than the design value can induce excessive concentration of plastic deformations with premature fracture in case of partial strength joints, or impair the response of those joints theoretically designed as full strength. These issues are crucial for seismic applications but are also very important under column loss scenarios. The robustness of a steel structure is highly influenced by the response of its joints, as highlighted by several experimental and numerical studies recently carried out on steel structures undergoing progressive collapse at the occurrence of a column loss scenario (Izzudin *et al*. 2008, Yang and Tan 2013, Sadek *et al*. 2013, Huvelle *et al*. 2015, Dinu *et al*. 2015, 2016, Cassiano *et al*. 2016, 2017, Tartaglia and D'Aniello 2017). These studies also highlighted that the presence of inner bolt rows (namely located in the center of the connection) can improve the resistance of the joint under catenary actions, by providing an increased rotational capacity under column loss scenario. In case of ESEPB joints, the bolt-rows are generally located very close to the beam flanges in order to maximize the lever arm and to guarantee the transfer mechanism of tensile forces from the beam flange to the column. Indeed, under shear forces and bending moments, the inner bolt rows are mostly inactive, especially those located in the middle of the connection (i.e., close to the neutral axis of the beam). In light of this consideration, ANSI/AISC 358-16 (2016) does not require the presence of inner bolt rows close to the center of the connection for seismically pre-qualified ESEPB joints. However, the presence of a bolt row in the middle axis of the connection can reduce the gap opening of partial strength connections under large rotational levels and can improve the robustness in case of catenary actions. Other parameters, such as the width among the bolts per row, the pitch between the bolt rows, the edge distance of the bolts, etc., can also affect the joint response. However, their effects can be easily accounted for in the design stage by means the component method. In addition, they are also scarcely prone to appreciable constructional defects. These considerations motivated the numerical study described and discussed in this paper, which aims at investigating: (i) the influence of the end-plate yield stress when it is different from the design value; and (ii) the presence of an additional bolt row in the center

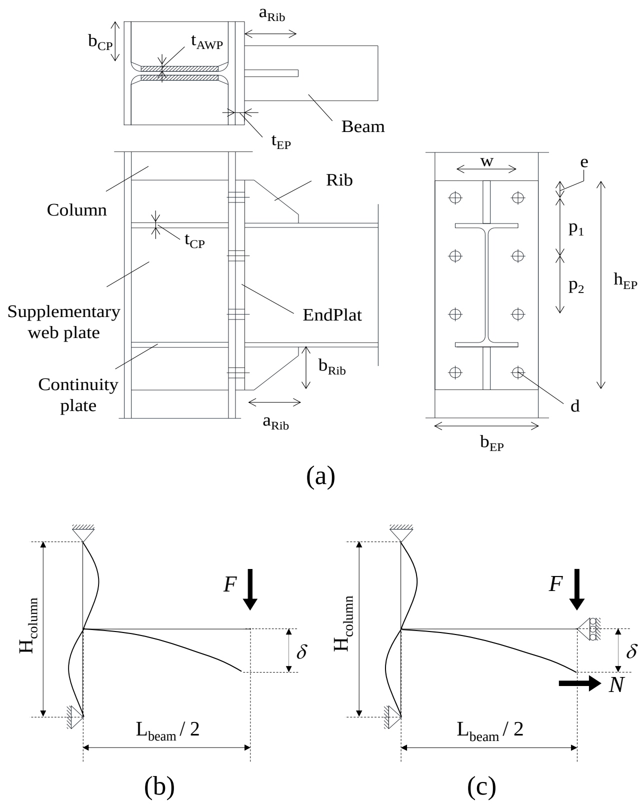

Fig. 1 Geometrical features of the examined joints (a); Sub-structuring and boundary conditions for FEAs under seismic actions (b) and column loss loading (c)

Table 1 Features of the designed joints

Joint ID	Performance level	End-plate			Rib		Bolts						Continuity plates		Supplementary web plate	
		h_{EP}	b_{EP}	t_{EP}	b_{Rib}	a_{Rib}	$n°$	d	e	w	p_1	p_2	b_{CP}	t_{CP}	Side	t_{SWP}
		mm	mm	mm	mm	mm	-	mm	mm	mm	mm	mm	mm	mm	-	mm
ES1-F	Full strength	760	260	25	200	235	12	30	50	150	75	160	222	14	2	8
ES1-E	Equal strength	600	280	18	120	140	8	27	50	160	160	180	222	14	1	8
ES1-P	Partial strength	600	280	16	120	140	8	27	50	140	160	180	222	14	-	-
ES2-F	Full strength	870	280	25	210	250	12	30	50	150	75	180	234	15	2	10
ES2-E	Equal strength	770	300	20	160	190	8	30	55	160	200	260	234	15	1	8
ES2-P	Partial strength	770	300	18	160	190	8	30	55	160	200	260	234	15	-	-
ES3-F	Full strength	1100	280	30	250	295	12	36	55	160	95	210	232	20	2	15
ES3-E	Equal strength	1100	300	22	250	295	8	36	55	160	95	210	232	20	1	15
ES3-P	Partial strength	1100	300	20	250	295	8	36	55	160	95	210	232	20	-	-

of the connection. The impact of these parameters on the local and global joint response is discussed with respect to cyclic actions and column loss induced effects. To this end, both monotonic and cyclic analyses were performed on a comprehensive set of joints designed according to D'Aniello *et al.* (2017b). However, concerning the strength of the end-plate material it is important to highlight that the aim of this study is not addressed to a reliability assessment but to examine the effectiveness of the design criteria violating intentionally the expected yield strength of the end-plate covering a possible range of variation.

The paper is organized in three main parts. In the first part, the design criteria of the joints and the investigated parametric variables are presented. In the second part, the modelling assumptions are described and validated against an experimental test carried out by the Authors. In the third part, the results obtained from finite element simulations are described and discussed.

2. Parametric finite element analyses

The beam-to-column assemblies constituting the examined joints were extracted from a set of reference buildings, designed according to EN1993:1-1 and EN1998-1. The selected beam-to-column assemblies are the following:

- beam IPE360 – column HEB280, labelled as "ES1";
- beam IPE450 – column HEB340, labelled as "ES2";
- beam IPE600 – column HEB500, labelled as "ES3".

Three joints were designed per beam-to-column assembly, namely one for each of the performance levels (i.e., full, equal and partial strength) defined by D'Aniello *et al.* (2017b) and implemented in the 2nd draft (v.2.1) of the EN 1993-1-8 under amendment. For clarity sake, full strength joints are designed to guarantee the occurrence of all plastic deformations in the beam; equal strength joints are characterized by the contemporary yielding of all macro-components (i.e., connection, web panel and beam) and partial strength joints are designed to develop plastic deformation only in the joint (connection and column web panel).The capacity design requirements to obtain the desired joint behavior can be guaranteed if the Eq.(1) is satisfied (D'Aniello *et al.* 2017b).

$$M_{wp,Rd} \geq M_{con,Rd} \geq M_{con,Ed} = \alpha \cdot (M_{B,Rd} + V_{B,Ed} \cdot s_h) \qquad (1)$$

$$M_{wp,Rd} = V_{wp,Rd} \cdot z \qquad (2)$$

In Eq. (1), $M_{wp,Rd}$ is the flexural strength corresponding to the capacity of column web-panel (see Eq. (2), $V_{wp,Rd}$ is the column web shear resistance, z is the internal level arm, $M_{con,Rd}$ is the flexural strength of the connection zone, $M_{con,Ed}$ is the design bending moment at the column face, $M_{B,Rd}$ is the design bending strength of the beam, $V_{B,Ed}$ is shear force corresponding to the occurrence of the plastic hinge in the connected beam, s_h is the distance between the applied shear and the column face. α depends on the design performance level andit is given by $\gamma_{sh}\times\gamma_{ov}$ for the full strength joints, while equal to 1 for equal strength joints and to 0.8 for partial strength joints (being γ_{sh} the hardening factor and γ_{ov} the ratio between the average and the characteristic yield stress of the steel).

In the case of dissipative connections (i.e., equal and partial strength configurations), a further hierarchy criterion was established by D'Aniello *et al.* (2017b) in order to avoid the failure of the bolts, so that the design tensile strength of each bolt row should be larger than the strength of the connected plate accounting for both the random variability of its yield stress and the relevant strain hardening. This requirement is expressed by Eq. (3), being d the nominal bolt diameter, γ_{M0} and γ_{M2} the partial safety factors according to Eurocode 3.

$$t \leq \frac{0.42 \cdot d}{\sqrt{\gamma_{ov} \cdot \gamma_{sh}}} \cdot \sqrt{\frac{\gamma_{M0} \cdot f_{ub}}{\gamma_{M2} \cdot f_y}} \qquad (3)$$

The main features of the designed reference joints (RJ) are shown in Fig. 1 and summarized in Table 1. All the investigated specimens have the same beam (L_{beam}) and

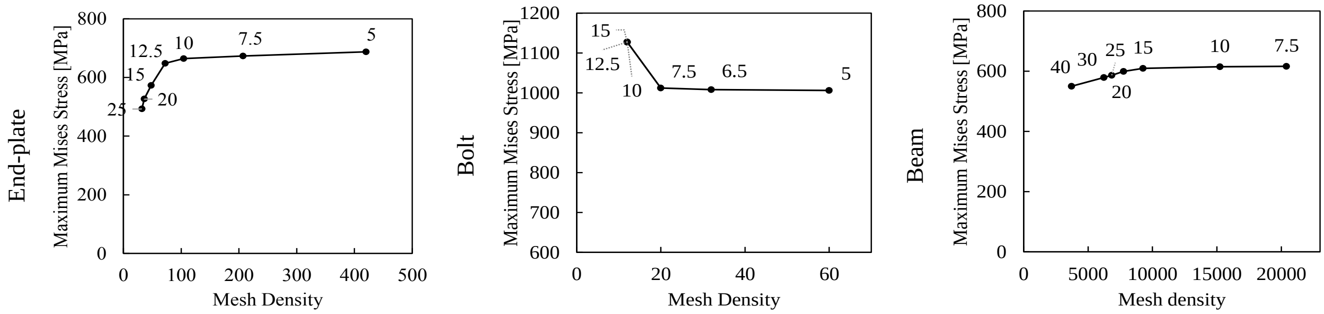

Fig. 2 Mesh sensitivity analysis results

column (H_{column}) length equal to 7m.Starting from these configurations, a wider range of joints was investigated by varying the following parameters:

- The yield strengthratio $\bar{f} = f_y / f_{y,d}$ (being f_y the actual yield stress and $f_{y,d}$ the design yield stress of the steel end-plate) was assumed equal to 0.65, 0.77, 1.00 and 1.30 (which corresponds to steel grades S235, S275, S355 and S460, respectively). The average yield stress for S355 (which is the reference material for the RJ) was set equal to $\gamma_{ov} \times f_y$ = 443.75 MPa (i.e., γ_{ov} = 1.25 according to EN1998-1).
- The presence of an additional inner bolt row located in the center of the connection (MBRJ).

The mechanical response of the joints was evaluated under monotonic and cyclic loading, in order to simulate the effects alternatively induced by horizontal forces acting on the building and sudden removal of the column.

3. Finite element modelling

3.1 Modelling assumptions

Finite element analyses (FEAs) were carried out using ABAQUS 6.14 (Dassault 2014). The models were discretized using C3D8I solid element type (i.e., 8-node linear brick, incompatible mode). In order to obtain regular element shapes the structured-meshing technique was employed and a mesh sensitivity analysis was performed to ensure the accuracy of the numerical model.

Fig. 2 depicts the peak Von Misses stress for ES1-F assembly (see Table 1) as respect to the mesh density (i.e., the number of finite elements per unit area) adopted for the end-plate, the bolts and the end segment of the beam (where plastic hinge is expected to form), since these parts are expected to develop the largest plastic strains. The numerical results show negligible improvement ofthe accuracy if the average global size of finite elements are smaller than 12.5, 10 and 15 mm respectively for the end-plate, the bolts and the beam-end. Therefore, the size of the elements adopted was kept equal or smaller than these dimensions throughout the numerical investigation.

The contacts between: (i) end-plate and column flange; (ii) bolt head and end-plate and nut and column flange; (iii) shank and the corresponding surface of the holes were

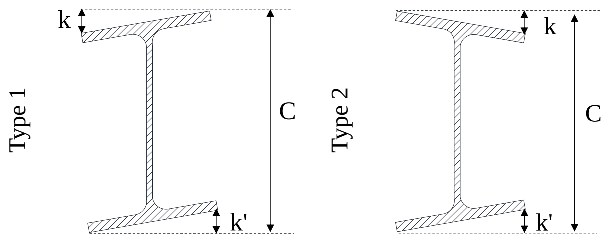

Fig. 3 Out-of-square shapes according to EN 10034

modelled by means of surface-to-surface interactions. Both normal and tangential contacts were used. The former was defined as "Hard Contact", which simulates the behavior perpendicular to the interface, both in case of pressure (overclosure) and gap opening (separation). The tangential behavior was simulated by means of the "Coulomb friction" model. The value of the friction coefficient was assumed equal to 0.3, which corresponds to steel surfaces cleaned by wire-brushing with loose rust removed according to EN1993:1-8 (2005).

The material used for beams, columns and plates corresponds to the European S355 steel with the average yield strength equal to $\gamma_{ov} \times f_y$. The Von Misses yielding criterion was used together with combined (i.e., both isotropic and kinematic) plastic hardening model based on Dutta *et al*. 2010.

The geometrical imperfections of steel members due to mill tolerances allowed by EN 10034 (1993) for European profiles were accounted for imposing the scaled shape of Eigen modes obtained by an elastic buckling analysis. Preliminary FEM analyses on cantilever beams were performed to select the type of the out-of-square buckling mode (e.g., Type 1 or Type 2 depicted in Fig. 3) leading the most severe condition (Tartaglia *et al*. 2018a, b). The response curves depicted in Fig. 4 in terms of the ratio between the bending moment at the column face (M_{cf}) and the beam plastic resistance ($M_{pl,\text{Beam}}$) show that the difference between the out-of-square typologies does not significantly influence the beam moment rotation curve for all investigated beams (i.e., IPE360, IPE450 and IPE600).

High strength (gr.10.9) pre-loadable HR bolts were used. The material properties of the bolts were defined by means of a multilinear force-displacement curve covering the initial elastic, yielding and plastic domain up to failure according to D'Aniello *et al*. (2016, 2017a). In addition, the shank necking and fracture in the threaded area has been

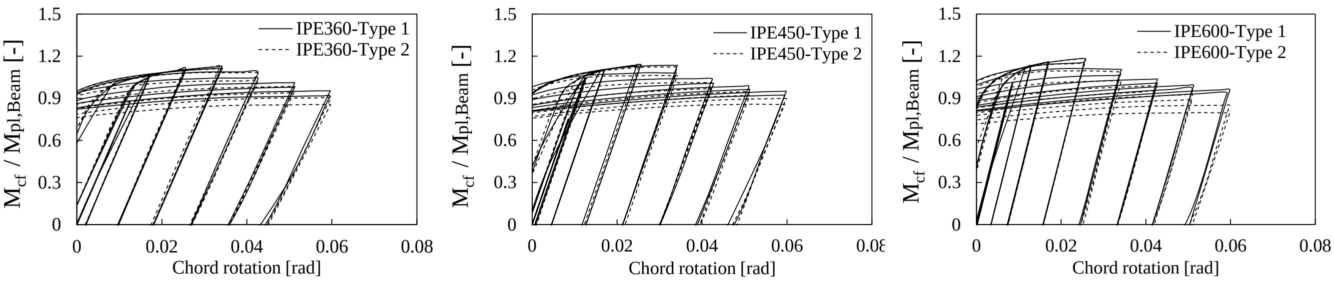

(a) IPE360 (b) IPE450 (c) IPE600

Fig. 4 Cyclic response of the cantilever beam considering the two out-of-square shapes according to EN 10034

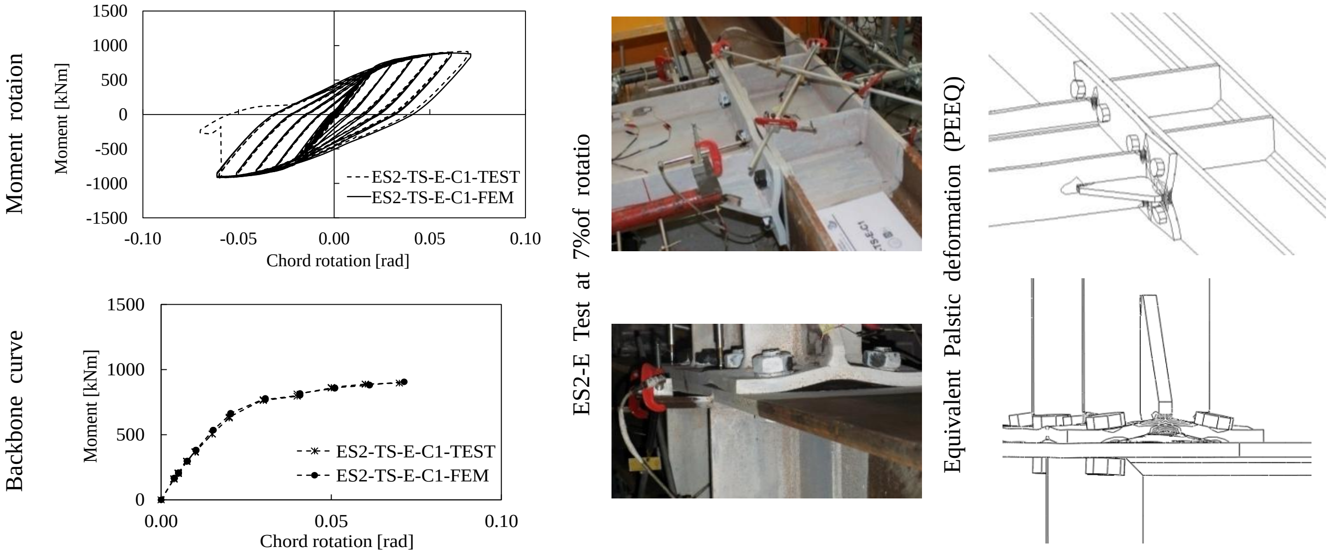

Fig. 5 Comparison between experimental results and finite element simulations: ES2-E

modelled using the ductile damage model, available in the software library, calibrated on the basis of Pavlovic *et al*. (2015) and D'Aniello *et al*. (2016 and 2017a).

The pre-tensioning of bolts was modelled in the first step of analysis (no applied external actions) using the "Bolt load" option available in the FE software and the clamping force was set equal to the values recommended by Eurocode 3 Part 1-8.

Both fillet and full penetration welds connecting the various elements and stiffeners were modelled. To ensure the continuity between the welded elements, the respective surfaces were connected by means of "Tie" constraints. The material of the welds was modelled by an elastic perfectly plastic constitutive law, with the yield stress equal to 460 MPa, which corresponds to an electrode grade A46 (as given by EN ISO 2560, 2009).

The boundary conditions were in accordance with the sub-structuring shown in Figs. 1(b) and (c). Torsional restraints were introduced out of the length of the plastic hinge. The spacing of lateral torsional restraints was assumed equal to the lateral-torsional stable length segment according to EN 1993-1 (2005), clause 6.3.5.3.Finally, the displacement histories were applied at the tip of the beam using dynamic implicit solver with quasi-static options.

3.2 Validation of modelling assumptions

The effectiveness of the modelling assumptions was validated against the experimental tests formerly carried out by Landolfo *et al*. (2017) on an equal strength (ES2-E) joint using the ANSI/AISC341-16 (2016) cyclic loading protocol up to a chord rotation equal to 0.07 rad. Fig. 5 shows that the modelling assumptions can capture with good approximation the resistance, the stiffness, the failure mode and the deformed shape experimentally obtained.

4. Discussion of results

4.1 Influence of end-plate material under monotonic and cyclic action

Fig. 6 shows the response curves of the joints under monotonic loading without axial restraints at the beam ends (see the structural scheme depicted in Fig. 1(b)) in terms of moment-joint rotation (i.e., the rotation computed considering the deformability of the connection and the column web panel) obtained by varying the material properties of the end-plate and compared with the beam

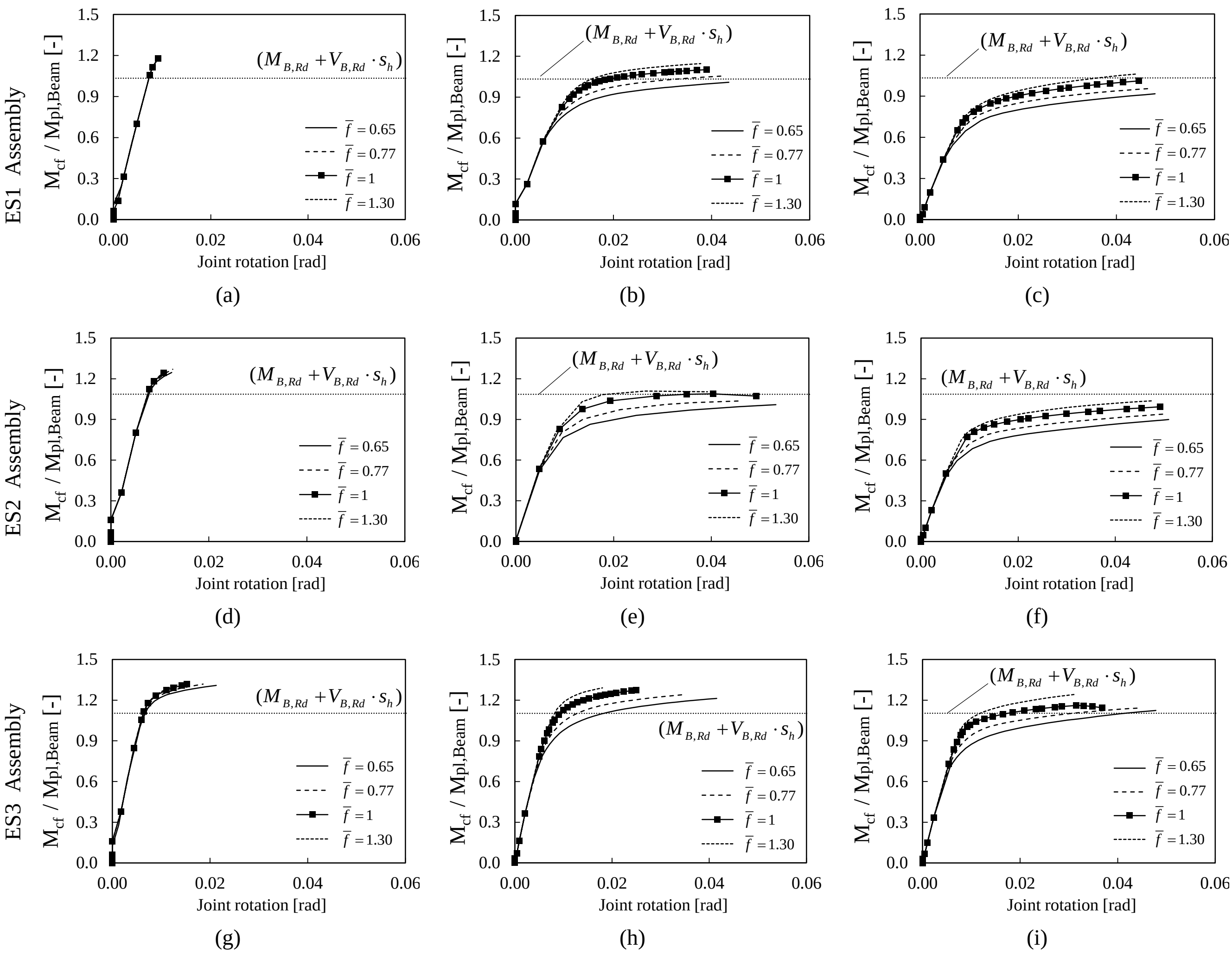

Fig. 6 Moment-joint rotation response curves varying the yield stress of the end-plate material: full strength (a, d and g), equal strength (b, e and h) and partial strength joints (c, f and i)

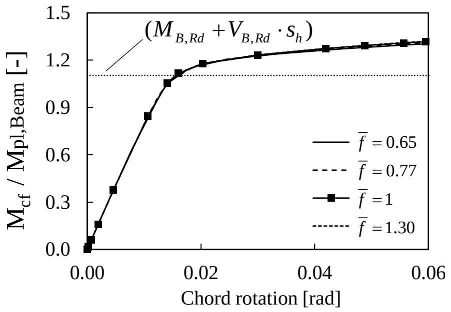

Fig. 7 Moment chord rotation curves for ES3-F

flexural strength at column face (i.e., $M_{B,Rd}$+$V_{B,Ed} \cdot s_h$).

The overall response curves of full strength joints (see Figs. 6(a), (d) and (g)) are less affected by the variation of the end-plate yield stress, thus confirming that the design rules proposed by D'Aniello *et al*. (2017b) are effective to guarantee the formation of plastic hinge into the beam. However, the local response shows some differences. In particular, for the same chord rotation level, the joint rotational demand differs varying the end-plate yield stress.

The ES3 assembly (i.e., which has the deeper beam) clearly highlights that for the same overall moment-chord rotation curve (see Fig. 7) corresponds different plastic demand in the joint, i.e., connection and column web panel, (see Fig. 8), which depends on the considered steel strength of the end-plate. As expected, the joint rotation decreases with the yield strength of the end-plate due to the formation of plastic deformations in the connection. To clarify this aspect, it is possible to take as an example the ES3-F assembly. In this case, the maximum PEEQ index in the beam at 6% chord rotation varies from 0.1445 to 0.1398 for end-plate steel grades ranging from S235 to S460, respectively (see Fig. 8). Conversely, the corresponding maximum PEEQ in the EP ranges from 0.0205 (for S235) to 0.00233 (for S460).

Equal strength joints are very sensitive to the variation of the steel strength of end-plate. This type of joints is theoretically designed to activate plastic deformations in both the beam and the end-plate. Of course, the adopted design procedure accounts for the variation of yield stress of end-plate, but when the deviation largely exceeds the values considered in the design procedure, the equal strength joints can alternatively tend to behave as either full

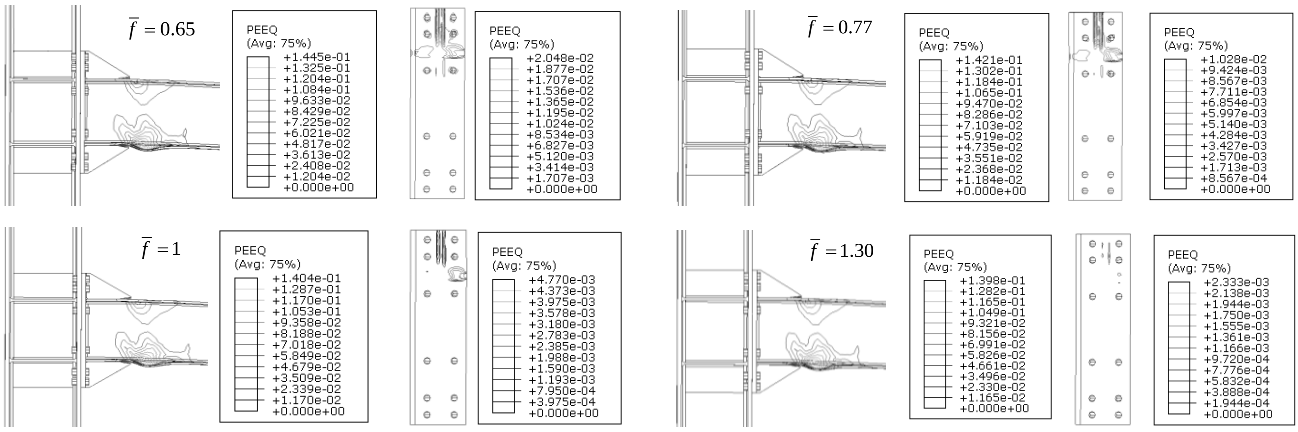

Fig. 8 PEEQ distribution for ES3 full strength joints varying the yield stress of the end-plate material

or partial strength joints. However, the results from FEAs confirmed that if the end-plate strength varies within the range of ± 30% of the design yield stress, the adopted capacity design criteria are effective to obtain the expected performance, namely plastic deformations in both beam and end-plate connection even though with different contributions. With this regard, FEAs show that two different damage patterns can occur: (1) first plastic hinge into the beam; subsequently plastic deformations with typical yielding lines occur into the end-plate due to hardening of the beam plastic hinge; (2) plastic deformations initiate into the end-plate; subsequently plastic hinge also forms into the beam due to the hardening of the end-plate (see Fig. 6).

On the other hand, increasing the strength of the end-plate modifies the failure mode of the bolt-rows from a ductile mode 1 to the brittle failure mode 3. Hence, in order to quantify the proneness of partial strength joints to fracture, the rupture index (*R*I) was monitored.

$$RI = \alpha \frac{PEEQ}{\varepsilon_f} = \frac{PEEQ}{\exp(-1.5T)} \tag{4}$$

The rupture index is defined as the ratio between the PEEQ and the ductile fracture strain ε_f, multiplied by the material constant α (El-Tawil *et al*. 1999), as in Eq. (4). Where the PEEQ value that causes fracture can be obtained for a given stress triaxiality condition T that is defined as the ratio between σ_H and σ_{eq}, which are defined according to Eqs. (5) and (6).

$$\sigma_H = \frac{\sigma_{xx} + \sigma_{yy} + \sigma_{zz}}{3} \tag{5}$$

$$\sigma_{eq} = \sqrt{\frac{(\sigma_{xx} - \sigma_{yy})^2 + (\sigma_{yy} - \sigma_{zz})^2 + (\sigma_{zz} - \sigma_{xx})^2 + 6(\tau_{xy}^2 + \tau_{yz}^2 + \tau_{zx}^2)}{2}} \tag{6}$$

Fig. 9 shows the relation of the RI with the chord rotation for different values of the yield stress of the end-plate material. For all the three beam-to-column assemblies (ES1, ES2 and ES3) the control point was selected in the middle axis of the end-plate, where the maximum value of the PEEQ was observed. As expected, the end-plate RI decreases for increasing yield strength and with the increase of the joint assembly dimensions. Therefore, the maximum value is observed for the ES1-P corresponding to the material configuration. This result highlights that an end-plate yield stress lower than the design value can significantly impair the response of partial strength joints due to the increase of RI indexes into the welded zones of the end-plate which can be prone to brittle failure.

The response of the bolts was also monitored, and the bolt forces were compared with those analytically estimated with the component method (CM) in accordance with the assumptions reported by D'Aniello *et al*. (2017b). With this regard, only the bolt rows above the symmetry axis were considered in tension since the others do not provide appreciable contribution.

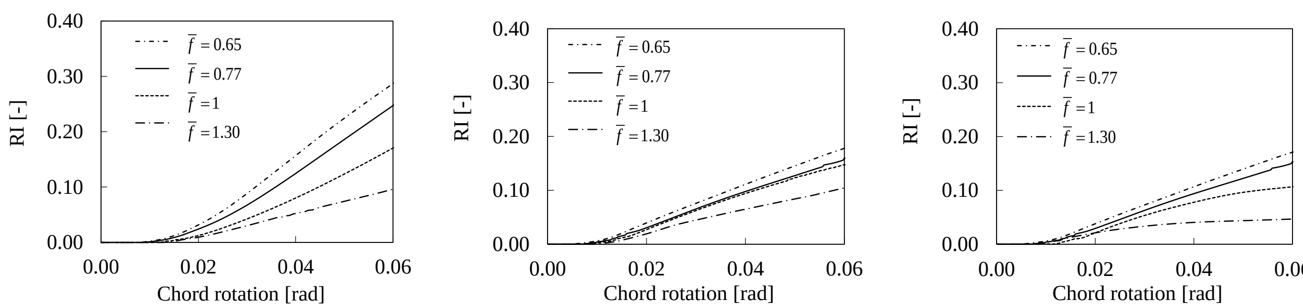

(a) End-plate (b) Bolt (c) Beam

Fig. 9 Evolution of Rupture Index with the chord rotation: ES1-P(a), ES2-P (b) and ES3-P (c)

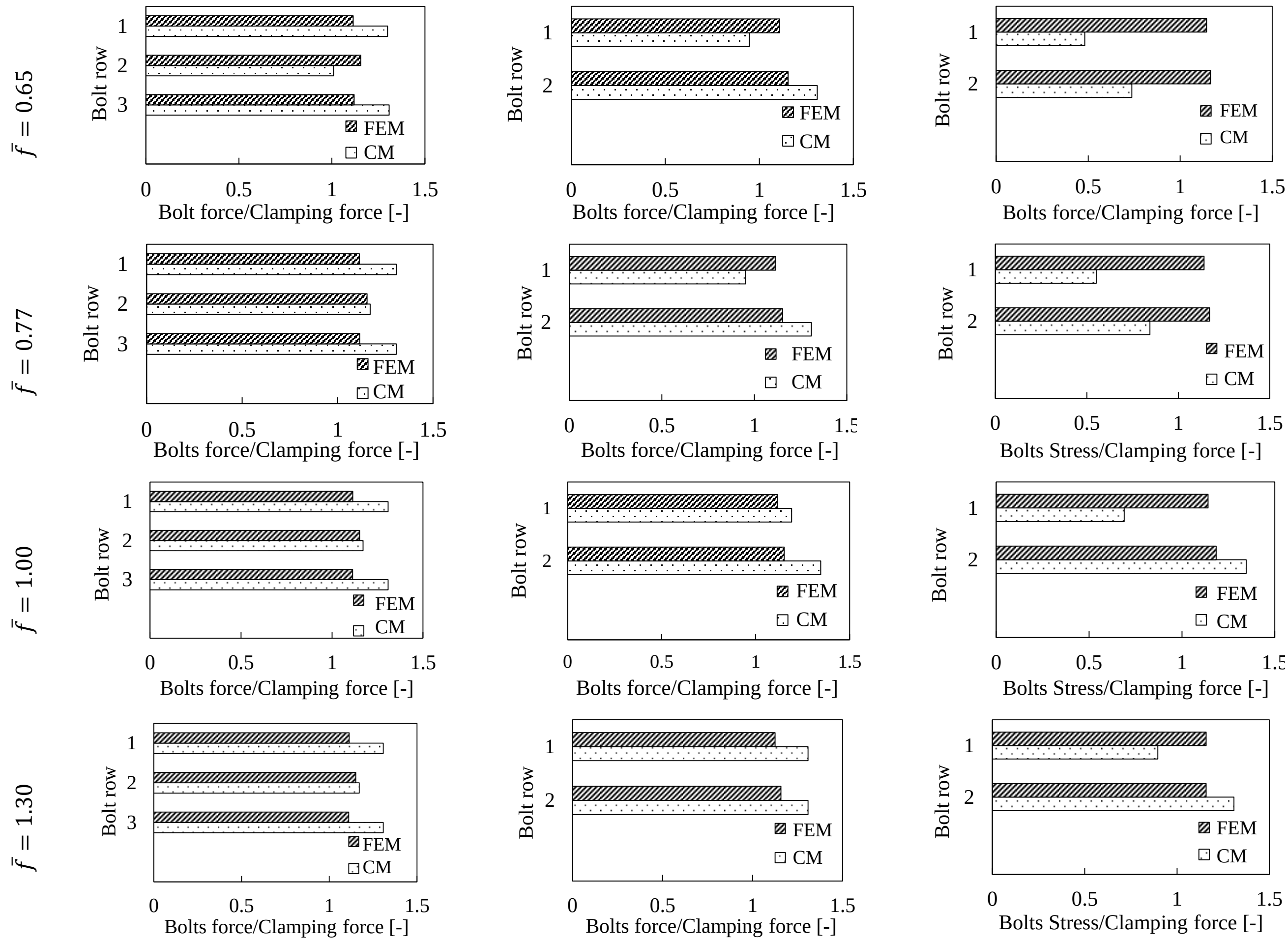

Fig. 10 Bolt Forces at 4% of chord rotation: FEM result vs CM prediction

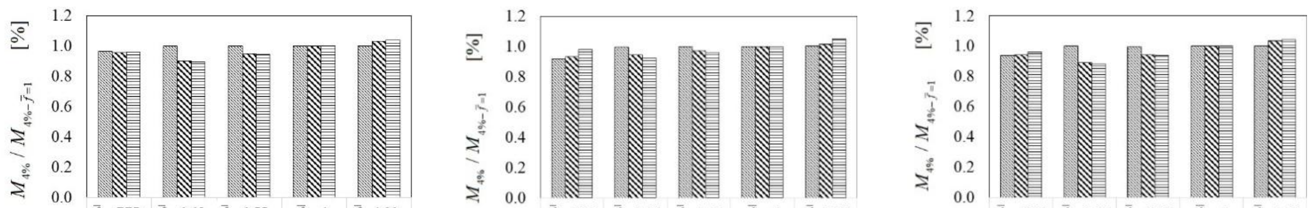

(a)	$\bar{f}$ = EEP	$\bar{f}$ = 0.65	$\bar{f}$ = 0.77	$\bar{f}$ = 1	$\bar{f}$ = 1.30
FULL	0.96	1.00	1.00	1.00	1.00
EQUAL	0.96	0.90	0.95	1.00	1.03
PARTIAL	0.96	0.90	0.94	1.00	1.04

(b)	$\bar{f}$ = EEP	$\bar{f}$ = 0.65	$\bar{f}$ = 0.77	$\bar{f}$ = 1	$\bar{f}$ = 1.30
FULL	0.91	0.99	1.00	1.00	1.00
EQUAL	0.93	0.94	0.97	1.00	1.01
PARTIAL	0.98	0.93	0.96	1.00	1.05

(c)	$\bar{f}$ = EEP	$\bar{f}$ = 0.65	$\bar{f}$ = 0.77	$\bar{f}$ = 1	$\bar{f}$ = 1.30
FULL	0.94	1.00	1.00	1.00	1.00
EQUAL	0.94	0.89	0.94	1.00	1.04
PARTIAL	0.96	0.89	0.94	1.00	1.05

(a) (b) (c)

Fig. 11 Bending moments at 4% of chord rotation: (a) ES-1; (b) ES-2; and (c) ES-3

Accordingly, the first three lines were investigated in the case of full strength assemblies, while only the first two lines were considered for the equal and partial strength joints. As depicted in Fig. 10, the bolt forces and their distribution at 4% of chord rotation obtained from FEAs differ from those analytically estimated. Nevertheless, it is interesting to observe that full strength joints do not exhibit appreciable differences of bolt forces at varying the end-plate material both in the FE and analytical predictions.

Contrariwise, the analytical calculations for equal and partial strength joints show an increase of bolt forces if the strength of the end-plate material increases, while the FEM results show negligible differences. Focusing on the partial strength assembly, it is possible to observe that by increasing the end-plate material resistance from $\bar{f} = 0.65$ to $\bar{f} = 1$, the bolt forces in both lines increase around 15%.

However, no differences can be pointed out between the configurations having $\bar{f} = 1$ and $\bar{f} = 1.3$. In this case, the increase of the end plate material resistance, changes the failure mode from the end-plate to the column flange, without significantly changing the forces in the bolts.

An overview of the sensitivity of the joint cyclic performance to the end-plate material is reported in Fig. 11, which compares the joint flexural resistance at a rotation of

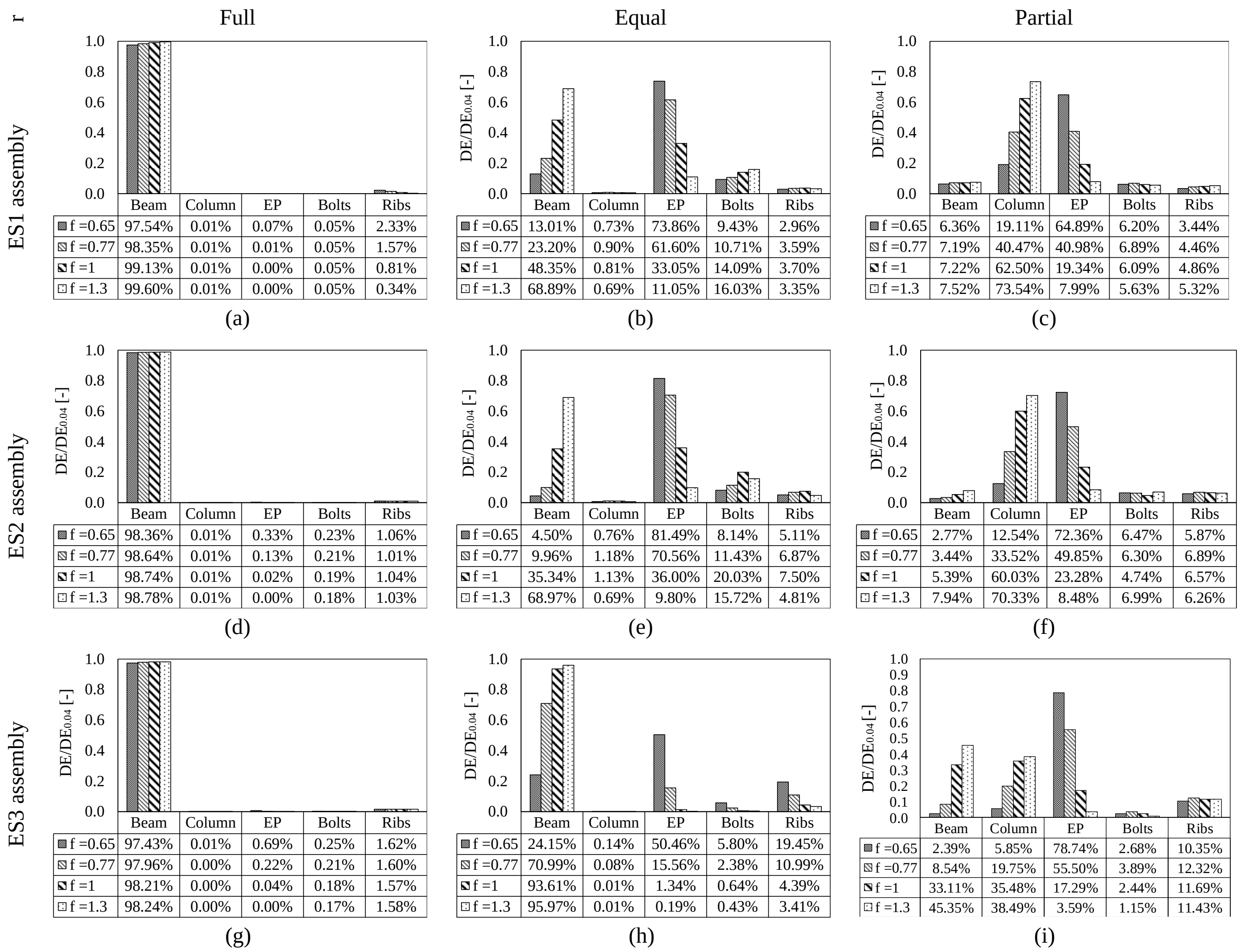

(a)

	Beam	Column	EP	Bolts	Ribs
f =0.65	97.54%	0.01%	0.07%	0.05%	2.33%
f =0.77	98.35%	0.01%	0.01%	0.05%	1.57%
f =1	99.13%	0.01%	0.00%	0.05%	0.81%
f =1.3	99.60%	0.01%	0.00%	0.05%	0.34%

(b)

	Beam	Column	EP	Bolts	Ribs
f =0.65	13.01%	0.73%	73.86%	9.43%	2.96%
f =0.77	23.20%	0.90%	61.60%	10.71%	3.59%
f =1	48.35%	0.81%	33.05%	14.09%	3.70%
f =1.3	68.89%	0.69%	11.05%	16.03%	3.35%

(c)

	Beam	Column	EP	Bolts	Ribs
f =0.65	6.36%	19.11%	64.89%	6.20%	3.44%
f =0.77	7.19%	40.47%	40.98%	6.89%	4.46%
f =1	7.22%	62.50%	19.34%	6.09%	4.86%
f =1.3	7.52%	73.54%	7.99%	5.63%	5.32%

(d)

	Beam	Column	EP	Bolts	Ribs
f =0.65	98.36%	0.01%	0.33%	0.23%	1.06%
f =0.77	98.64%	0.01%	0.13%	0.21%	1.01%
f =1	98.74%	0.01%	0.02%	0.19%	1.04%
f =1.3	98.78%	0.01%	0.00%	0.18%	1.03%

(e)

	Beam	Column	EP	Bolts	Ribs
f =0.65	4.50%	0.76%	81.49%	8.14%	5.11%
f =0.77	9.96%	1.18%	70.56%	11.43%	6.87%
f =1	35.34%	1.13%	36.00%	20.03%	7.50%
f =1.3	68.97%	0.69%	9.80%	15.72%	4.81%

(f)

	Beam	Column	EP	Bolts	Ribs
f =0.65	2.77%	12.54%	72.36%	6.47%	5.87%
f =0.77	3.44%	33.52%	49.85%	6.30%	6.89%
f =1	5.39%	60.03%	23.28%	4.74%	6.57%
f =1.3	7.94%	70.33%	8.48%	6.99%	6.26%

(g)

	Beam	Column	EP	Bolts	Ribs
f =0.65	97.43%	0.01%	0.69%	0.25%	1.62%
f =0.77	97.96%	0.00%	0.22%	0.21%	1.60%
f =1	98.21%	0.00%	0.04%	0.18%	1.57%
f =1.3	98.24%	0.00%	0.00%	0.17%	1.58%

(h)

	Beam	Column	EP	Bolts	Ribs
f =0.65	24.15%	0.14%	50.46%	5.80%	19.45%
f =0.77	70.99%	0.08%	15.56%	2.38%	10.99%
f =1	93.61%	0.01%	1.34%	0.64%	4.39%
f =1.3	95.97%	0.01%	0.19%	0.43%	3.41%

(i)

	Beam	Column	EP	Bolts	Ribs
f =0.65	2.39%	5.85%	78.74%	2.68%	10.35%
f =0.77	8.54%	19.75%	55.50%	3.89%	12.32%
f =1	33.11%	35.48%	17.29%	2.44%	11.69%
f =1.3	45.35%	38.49%	3.59%	1.15%	11.43%

Fig. 12 Dissipated energy by the components of ES1 ((a)-(c)), ES2 ((d)-(f)) and ES3 ((g)-(i))

4% normalized with respect to the bending capacity of the reference joint (in which the S355 is assumed as the end-plate material).Indeed, the energy dissipated by the end-plate (see Fig. 12) varies from about 80 to 10% of the total amount for $\bar{f}$ ranging from 0.65 to 1.3. However, despite this difference, the energy dissipation of equal strength joints is mostly distributed between the end-plate and the beam, thus consistently with the design requirements D'Aniello *et al.* (2017b). The energy dissipated by the bolts is quite low in all the examined cases (see Fig. 12). This outcome confirms the effectiveness of the design hierarchy criteria in guaranteeing a ductile response. However, partial strength joints can experience excessively large deformation of the column for $\bar{f} = 1.3$ as respect to EC8 limit.

Fig. 13 shows the results in terms of moment-rotation curves, energy dissipation contributions and PEEQ distribution for the ES2-E, which clearly highlight how the damage pattern shifts from the end-plate to the beam when increasing the yield strength of the end-plate. Indeed, as shown in Fig. 12(e), the models with the weakest end-plate ($\bar{f} = 0.65$) develop most of the plastic demand in the end-plate (i.e., 81.5%), thus behaving as a partial strength joint. Increasing the yielding resistance of the end-plate material, the joint response tends to the full strength behavior, concentrating the plastic demand into the beam (i.e., 69%).

Moreover, also the cyclic analyses on partial strength joints show that $\bar{f}$ does not modify the dissipative mechanism. Indeed, in all cases, the hysteretic energy is dissipated by the connection and the column web panel, leaving almost elastic the other joint components (see Figs. 12(c), (f) and (i)). Despite the fact that a large part of the plastic deformation is concentrated into the end-plate, the contribution of the bolts does not exceed the 7% of the total dissipated energy. Therefore, even for this set of joints the design criteria proposed by D'Aniello *et al.* (2017b) are effective to limit brittle failure modes.

4.2 Influence on column loss response of end-plate material different from the design value

The column removal scenario implies the sudden loss of a column adjacent to the investigated joint (see Fig. 1(c)). In this case, the presence of axial restraints and the large deformation regime substantially modify the local demand in the joint components due to the development of catenary actions into the beam and the rotational demand is generally larger than the value expected under seismic conditions. Under the column loss, the column face bending moment

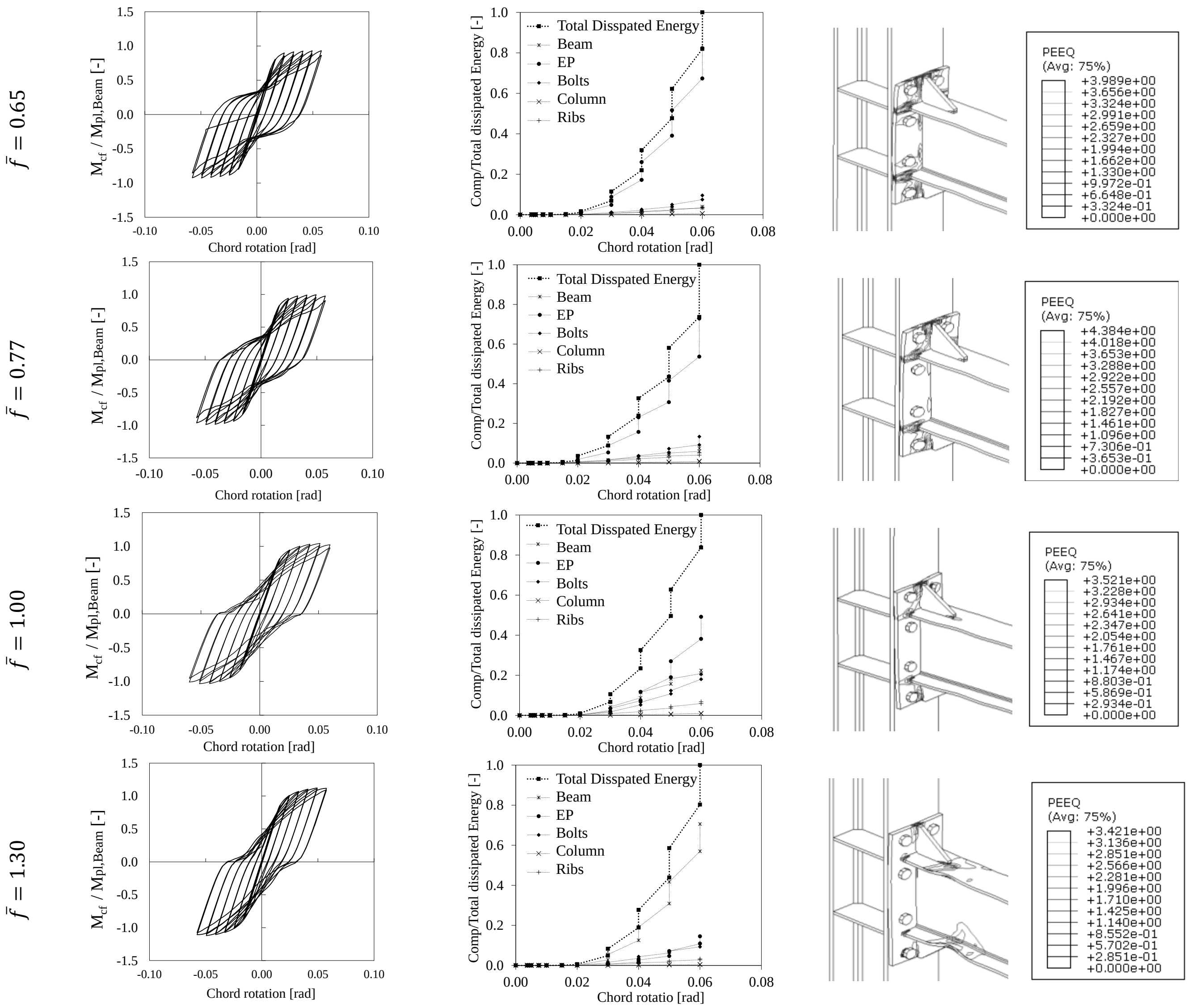

Fig. 13 Influence of the variation of steel strength of the end-plate on the response of ES2-E in terms of Moment - chord rotation curve, dissipated energy and PEEQ distribution

calculated with the first order theory (i.e., $M^I = F \cdot \delta$, being F and δ the applied force and the corresponding vertical displacement at the beam tip) does not correspond to the actual bending moment acting on the connection, which depends also on the additional contribution of the moment due to the axial tensile force in large deformation. Hence, the total bending moment at column face can be calculated using Eq. (7).

$$M_{cf} = M^I + M^{II} = M^I - N \cdot \delta \quad (7)$$

The catenary action developed in the examined full strength assemblies does not appreciably differ with the variation of the end-plate material and it ranges between the 20 and 35% of the plastic axial resistance of the beam ($N_{pl,Rd,\text{Beam}}$), as shown in Fig. 14.

ES1-F and ES2-F are scarcely influenced by the variation of the end-plate material showing a very ductile behavior although plastic hinges form in the column out of the web panel for chord rotation larger than 10% (see Fig. 14). Contrariwise, ES3-F shows a different failure mode with damage concentration into the connection and brittle rupture of the bolts (see Fig. 14).

For this case, the variation of the yield strength of the end-plate material appreciably influences the damage pattern at rotations larger than 10% (i.e., the threshold from which the progressive failure of bolts activates), but affecting less the joint response curve. The reason of the different response of the ES3-F depends on the tensile resistance of the bolts compared to the catenary action developing under column loss.Indeed, the tensile resistance of the bolts ($\Sigma F_{t,Rd}$) in the upper half part (i.e., above the symmetry axis) of the connection for ES1 and ES2 configurations is close to the plastic strength of the beam. Therefore, $\Sigma F_{t,Rd}/N_{pl,Rd,\text{Beam}}$is respectively equal to 0.96 and 1.00. On the contrary, the resistance of the bolts in the tensile part of the connection of ES3-F is significantly smaller, namely$\Sigma F_{t,Rd}/N_{pl,Rd,Beam} = 0.65$.These observations suggest that the effect of catenary action on the connection response can be disregarded at design stage if the tensile

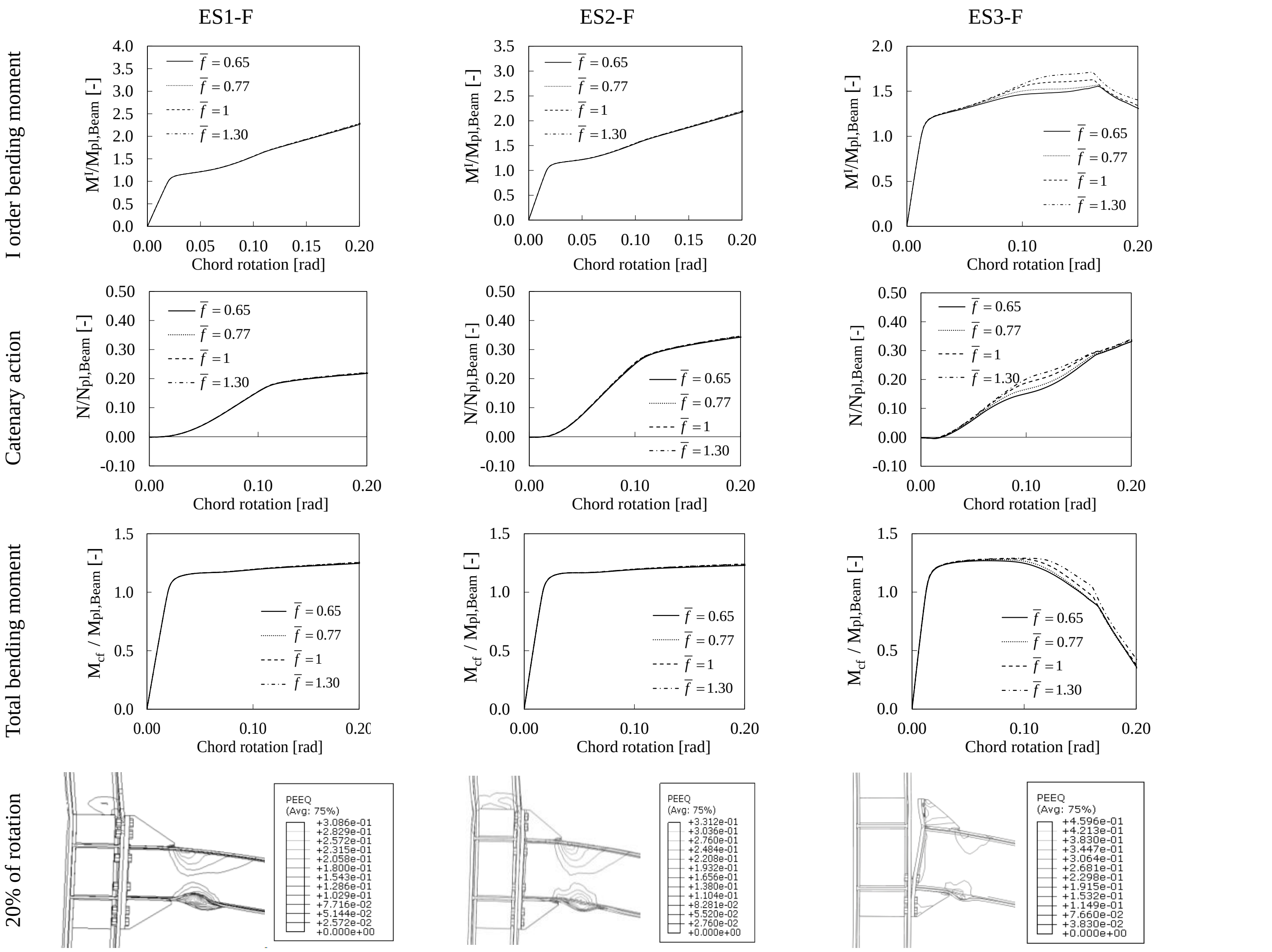

Fig. 14 Influence of the variation of the end-plate steel strength on the full strength joints under column loss scenario

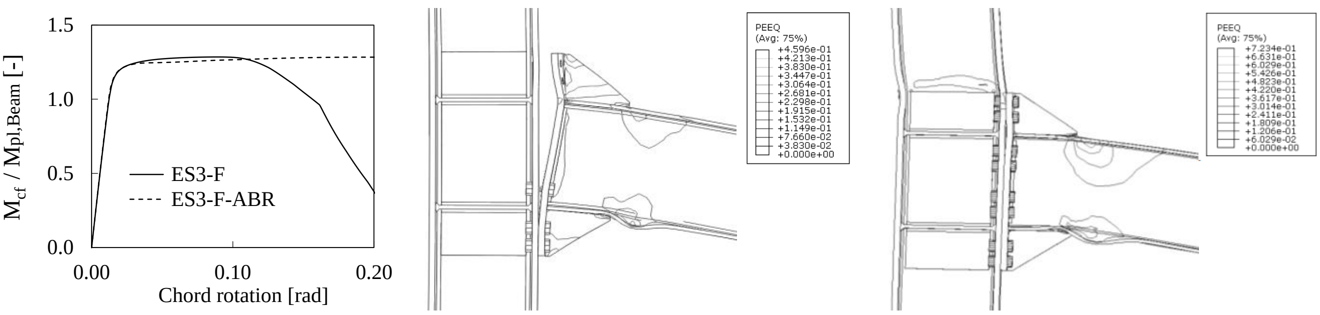

(a) (b) (c)

Fig. 15 ES3-F vs ES3-F-ABR in terms of moment-rotation curve (a) and yield line pattern ((b) and (c))

strength of the half part of the bolted connection is close to the tensile resistance of the connected beam. However, if the design objective is to avoid any type of damage in the column, the strength of the column web panel as well as the bending resistance of the column segments outside the joint should be properly verified against the expected catenary action.

In order to verify if the increase of resistance of the bolts ($\Sigma F_{t,Rd}$) in the tensile part of the connection is effective in improving the performance under column loss, the ES3-F was re-designed considering a 8-bolt row configuration, namely with two additional bolt rows (one more per beam flange).Under this assumption the new joint (identified as "ES3-F-ABR") is characterized by a larger $\Sigma F_{t,Rd}/N_{pl,Rd,Beam}$ ratio, which increases from 0.65 to 1.04.

Fig. 15 shows the comparison in terms of both moment-

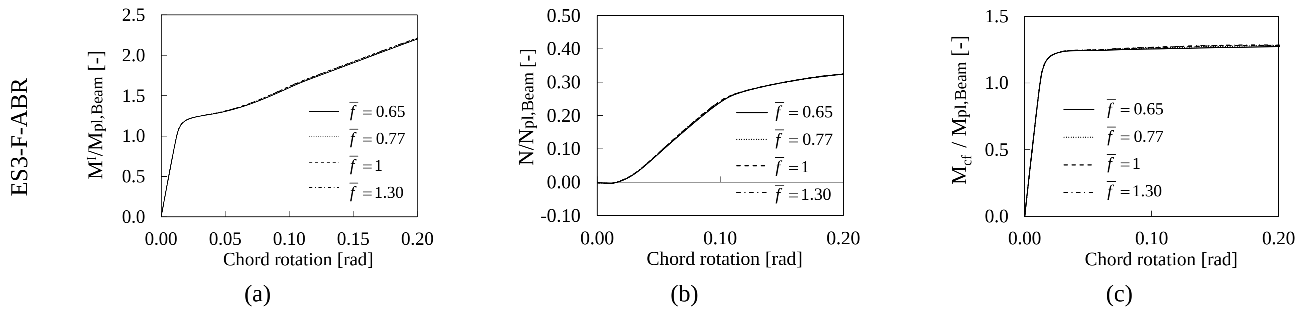

Fig. 16 Influence of the variation of the end-plate steel strength on the ES3-F-ABR behavior under column loss scenario in terms of: Ist order moment (a), catenary action (b) and total bending moment (c)

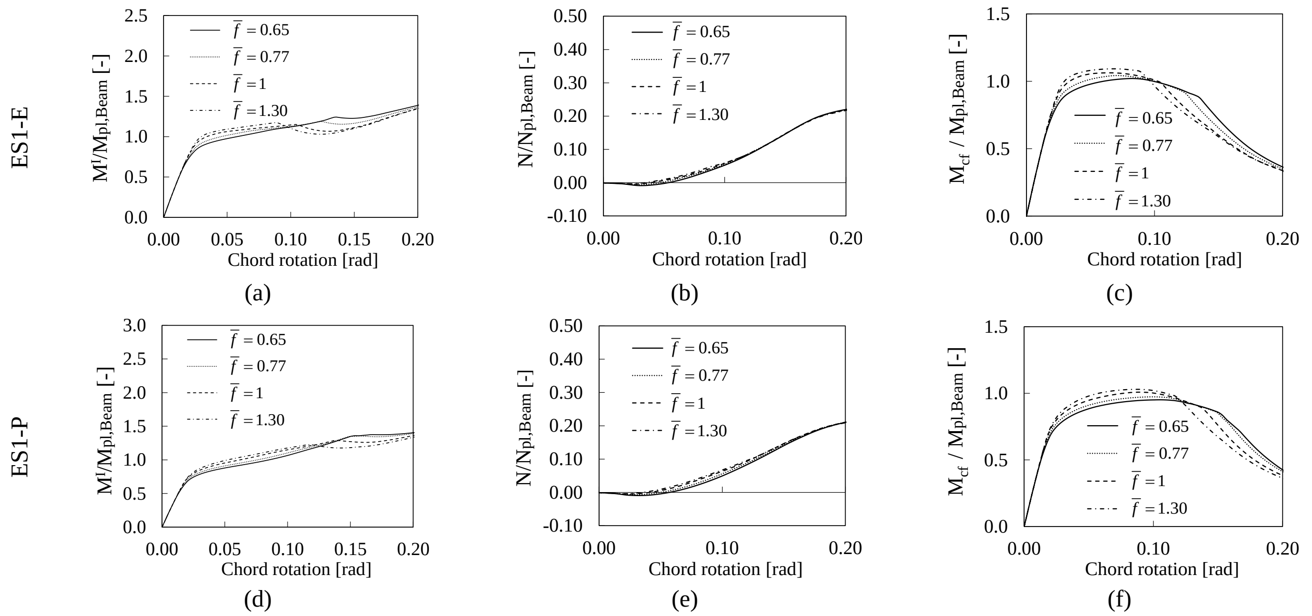

Fig. 17 Influence of the variation of the end-plate steel strength for ES1-E and ES1-P joints under column loss scen ario in terms of: I order moment (a, d), catenary action (b, e) and total bending moment (c, f)

rotation curve and PEEQ distribution between the ES3-F and the ES3-F-ABR, which confirms that the new detail can significantly improve the joint response. Hence, as expected, the ES3-F-ABR joint behavior is similar to the response observed for the ES1-F and ES2-F joints (see Figs. 16 and 18(a)) with the formation of the plastic hinges on both the beam and the column. Moreover, as depicted in Fig. 16 and consistently with the results shown for the ES1-F and ES2-F, the variation of the steel yield strength of the end-plate does not affect the global response of the joint. A minor difference between the two cases can be only observed at rotation equal to 20%, where the plastic deformation in the end-plate is slightly larger in the former case, without influencing the overall response of the joint.

The influence of the variation of the end-plate steel strength is more significant for equal and partial strength joints, as also shown in the previous paragraph. These joint configurations exhibit similar response under column loss without appreciable differences. Indeed, since these joints are designed to promote the yielding of the connection, the increase of the yield strength of the end-plate increases the joint bending capacity, but decreasing the ductility if the strength of the end-plate exceeds the resistance of the corresponding bolt rows. In that condition, the damage pattern in the connection moves from mode 2 to a mode 3, with plastic deformation occurring in the column at large rotation demand.

Fig. 17 shows the response curves of ES1-E in terms of first order moment-rotation (*a*), axial force (*b*), and second order moment (*c*) normalized to their relevant plastic resistances of the gross section (i.e., $M_{pl,\mathrm{Beam}}$ and $N_{pl,\mathrm{Beam}}$ for bending and axial strength, respectively). The connection with $\bar{f} = 0.65$ exhibits a failure mode 1 up to 10% of chord rotation (see Fig. 17(c), but increasing the rotational demand the catenary actions increases (Fig. 17(b) and the bolts fail under tension. Increasing the yield resistance of the end-plate material up to $\bar{f} = 1.3$, the bending capacity increases with a consequent larger stress concentration in the bolts up to their premature fracture at 10% of rotation.

However, all examined cases lose the first two bolt lines at rotation levels equal to 20% (see Fig. 18(b)), even though the distribution of plastic deformation significantly differs from the weaker to the stronger end-plate. Indeed, in the former case (i.e., $\bar{f} = 0.65$) the damage is mostly localized

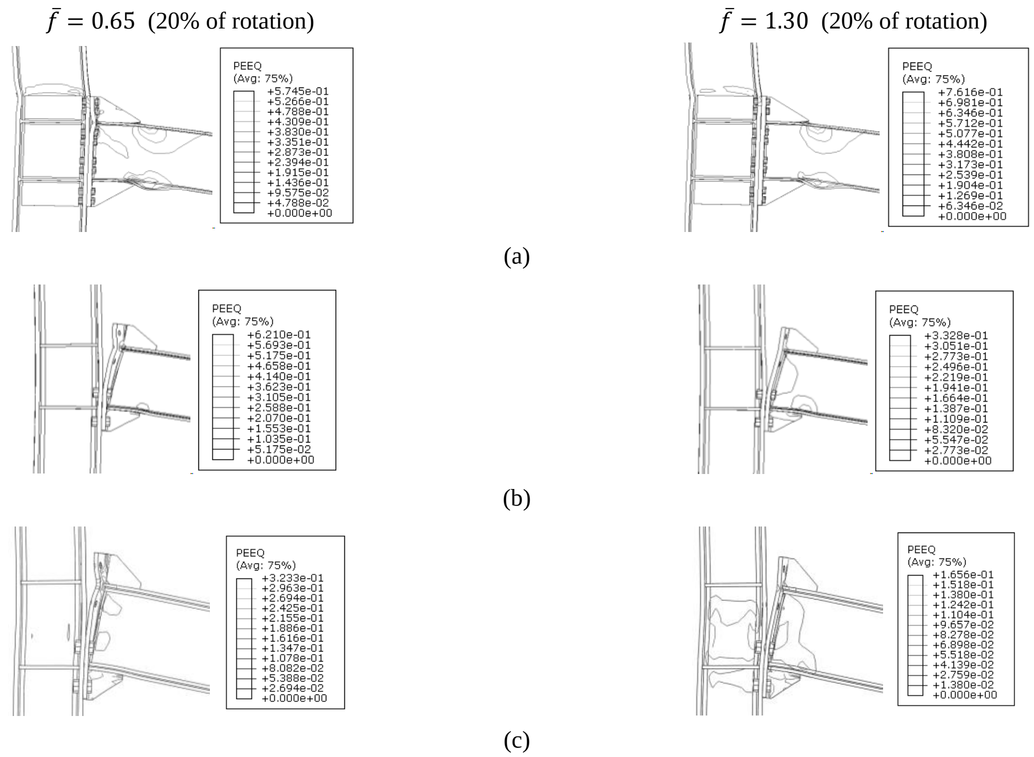

Fig. 18 PEEQ deformation at 10 and 20% of rotation of: ES3-F-ABR (a), ES1-E (b) and ES1-P (c)

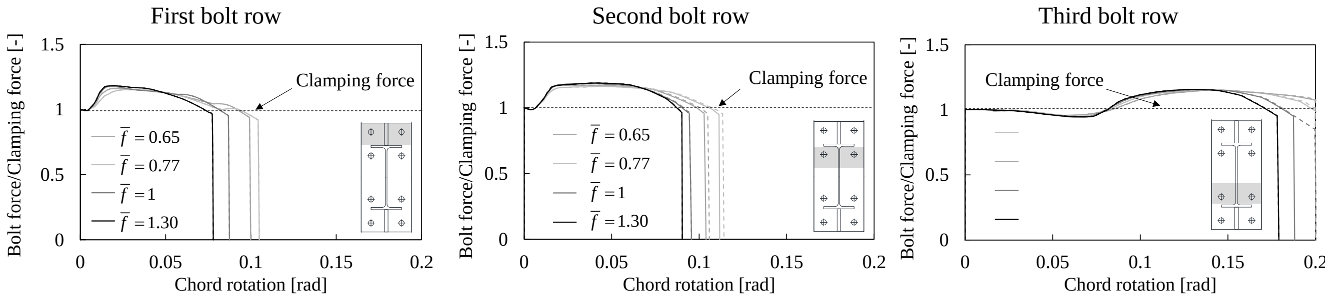

Fig. 19 ES1-P joints: Bolts force variation in function of the end-plate material variability

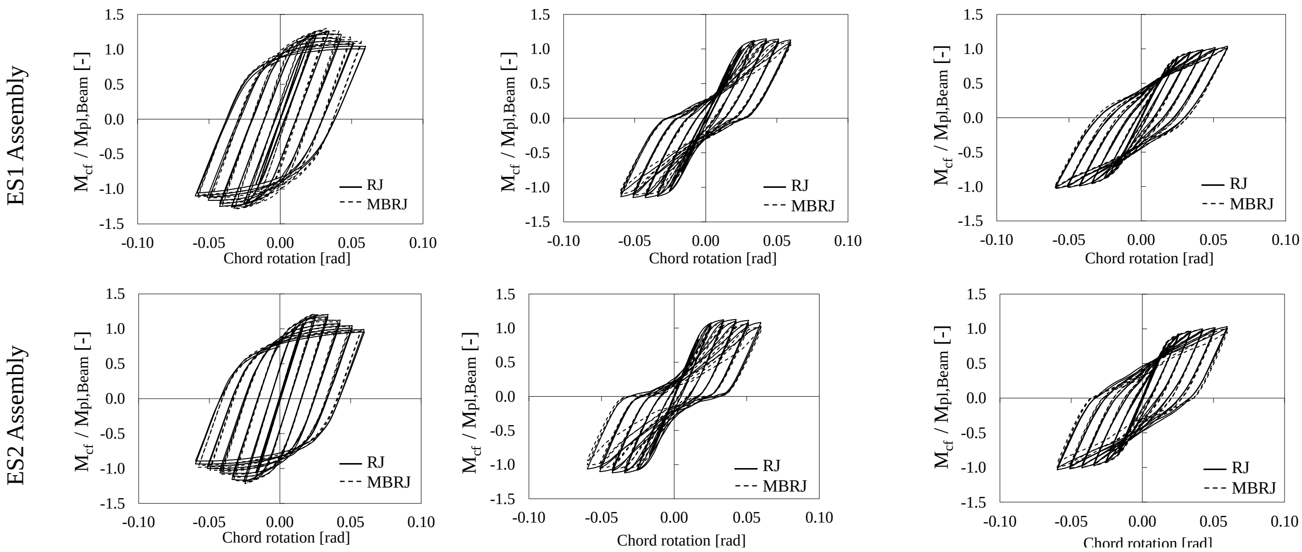

Fig. 20 Comparison between RJ and MBR in terms of cyclic moment-rotation curves

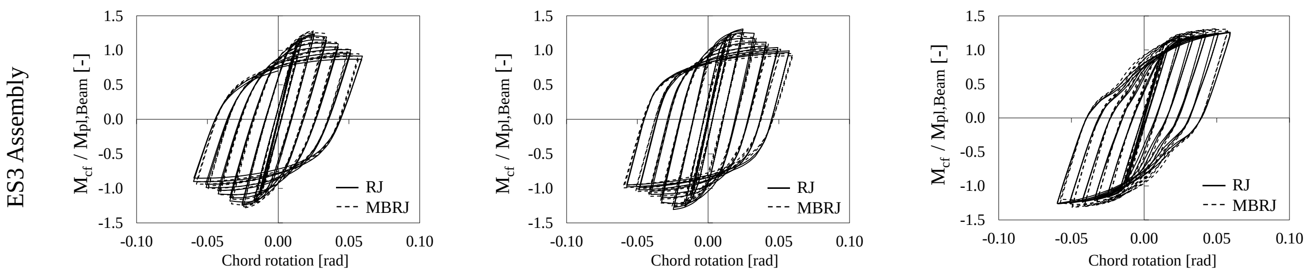

Fig. 20 Continued

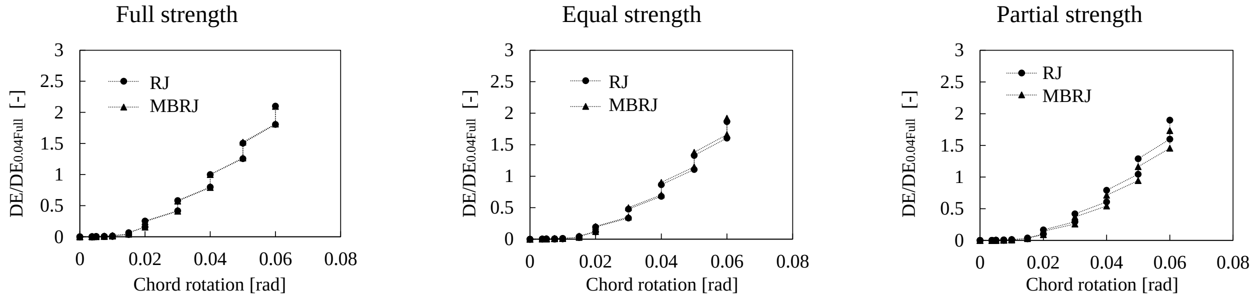

Fig. 21 Dissipated energy per cycle

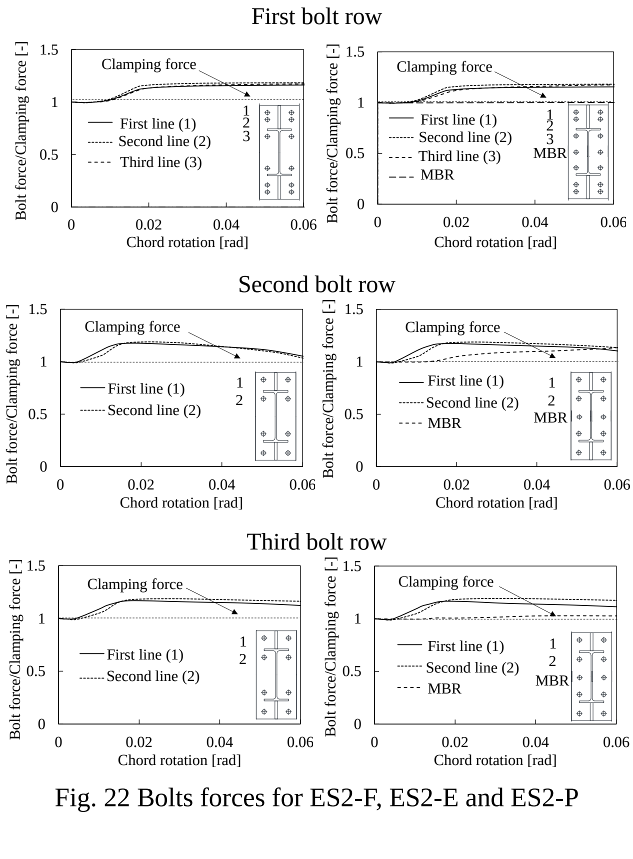

Fig. 22 Bolts forces for ES2-F, ES2-E and ES2-P

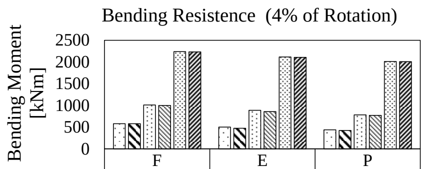

	F	E	P
ES1-MBRJ	578	500	438.5
ES1-RJ	578	473	423
ES2-MBRJ	1010	887	782
ES2-RJ	997	858	770
ES3-MBRJ	2240	2116	2012
ES3-RJ	2234	2107	2008

Fig. 23 RJ vs MBRJ in terms of bending resistance

in the end-plate and the welds between the beam web and the end-plate.

In the second case (i.e.,$\bar{f} = 1.3$) the plastic deformations mostly occur into the beam, the rib-to-beam flange welds and bolts, thus confirming the evolution of failure mode 2 (observed at 10%) into a mode 3. For the sake of brevity, the response of the other equal strength joints is not reported, since their response in terms of moment-rotation curve and failure mode is similar to that of ES1-E.

Figs. 17(d), (e) and (f) and Fig. 18(c) depict the response of ES1-P varying the resistance of the end-plate material. As for equal strength joints, the increase of $\bar{f}$ corresponds to an increase of bending resistance but it is also associated to an increase of plastic demand in the column web panel and a ductility reduction. Indeed, since partial strength joints are designed to yield in both column web panel and connection, increasing the end-plate material modifies the failure mode of the bolt rows from type 2 to type 3, as well as the plastic deformation demand in the column.

As observed, the behavior of the bolts plays a very important role in the definition of both the equal and partial strength joints behavior. Therefore, the bolt forces of each row normalized to their clamping forces were plotted against the chord rotation (see Fig. 19). Both the first and the second bolt rows show an increase of the tensile forces starting from the clamping up to their plastic strength. Despite the fact that all bolts reach almost the same level of force, the fracture occurs at different values of rotation in function of the end-plate material variation, namely the

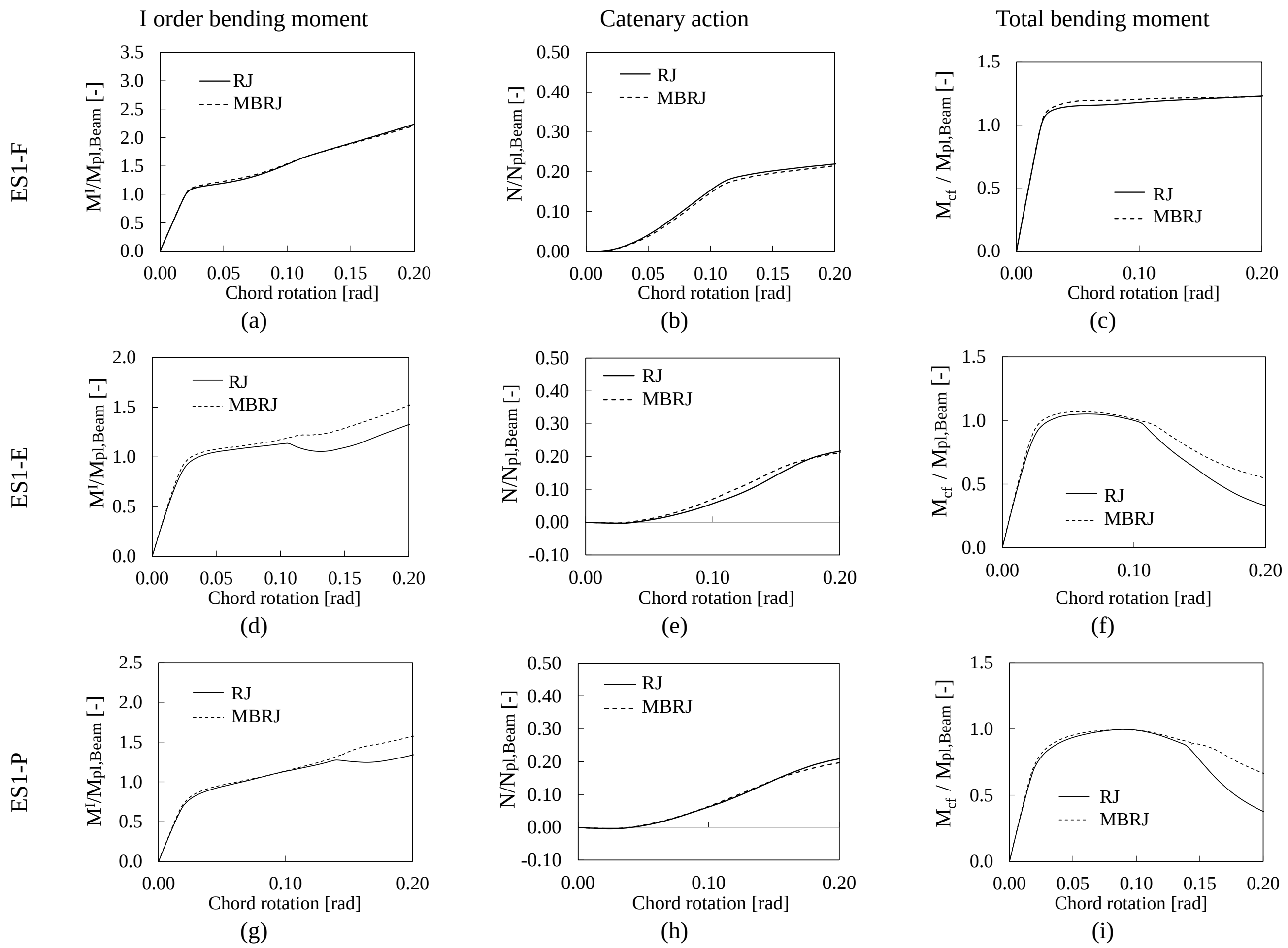

Fig. 24 Influence of central bolt row under column loss for ES1 full, equal and partial strength joints: first order moment chord rotation ((a), (d) and (g)), axial force ((b), (e) and (h)) and second order moment ((c), (f) and (i))

failure of the bolts anticipates with the increase of the resistance of the end-plate material, thus showing a consequent decrease of ductility. The third bolt row is under compression up to 8% of rotation. Further increasing the imposed rotation, the bolts of the first and second row fail, and this bolt row exhibit a similar dependency with the material strength of the end-plate.

4.3 Influence of a central bolt row

Fig. 20 depicts the comparison between the cyclic response curves of RJs and MBRJs. As it can be recognized, the hysteretic curves are mostly overlapped with small differences for the partial strength joints. This observation is also confirmed by Fig. 21, where the cumulated energy per cycle (DE) is depicted. DE was calculated per beam-to-column assembly as the ratio between the sum of the areas enclosed by each hysteretic loop and the energy cumulated up to 0.04 rad of chord rotation of the corresponding full strength joint ($D_{E0.04,Full}$). As expected, given that the plastic deformation concentrated solely into the beam, the response and the dissipated energy of full strength joints are insensitive to the presence of the additional bolt row. Larger differences can be observed in the case of partial strength joints where the presence of the central bolt row reduce the gap opening of the connection and, consequently, the corresponding pinching of the hysteretic response curve. As shown in Fig. 22, the central bolt row is not activated in the case of both full and equal strength joints, showing a constant reaction equal to the applied clamping force.

The comparison in terms of bending strength between the references joints (RJs), see Table 1, and the joints with an additional bolt row in the middle of the connection (MBRJs) is also summarized in Fig. 23, which clearly highlights that the differences between the response of the two configurations in terms of plastic strength at 4% of rotation are negligible.

Contrariwise, the central bolt row is activated in the case of partial strength joint at almost 1.8% of rotation. These results clearly highlight that the influence of the central bolt row is negligible for joints designed to resist solely the effects due to gravity and lateral loads, so that its use is not justifiable considering the increase of unitary constructional cost. The remarks previously detailed in the case of cyclic actions are controverted for column loss scenario. Indeed, the increase of tensile resistance of the connection is beneficial due to the development of catenary actions when the joints are subjected to large rotational demands (see Fig. 1(c)).

Fig. 24 shows the comparison between ES1-RJs an.

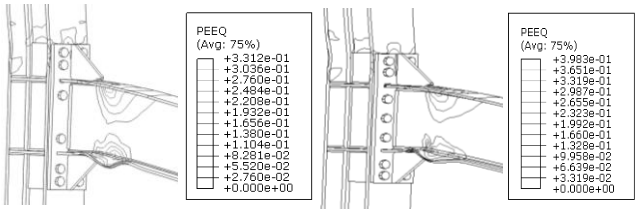

(a) ES1-F

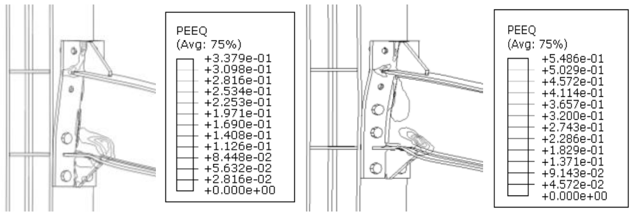

(b) ES1-E

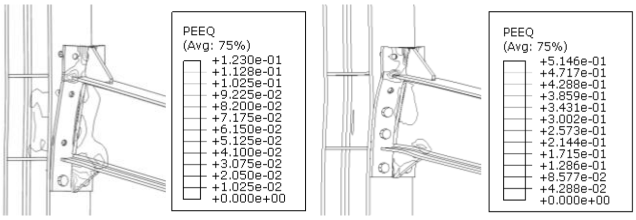

(c) ES1-P

Fig. 25 PEEQ distribution in ES1 assemblies

ES1-MBRJs in terms of moment-rotation (both first and second order) and axial force-rotation response curves. The two full strength joints show similar response (see Figs. 24(a), (b) and (c)). Indeed, both RJ and MBRJ initially develop the plastic hinge at the level of the beam end. Afterwards at 20% of chord rotation plastic deformations occur in the column at the upper part of the joint due to the development of catenary action (see Fig. 25(a)). This result shows that both configurations have enough connection tensile resistance to resist the catenary action, given that $\Sigma F_{t,Rd}/N_{pl,Rd,\mathrm{Beam}}$ is equal to 0.96 and 1.28, respectively.

The response of both equal and partial strength joints is highly influenced by the presence of the central bolt row (see Figs. 24(d)-(i)). Indeed, the central bolt row allows increasing the strength and the joint ductility, limiting the gap opening of the connection and the bolt fracture (see Figs. 25(b) and (c)). This observation is also confirmed by monitoring the force developed in the bolts. Fig. 26 shows the comparison between the bolt forces per active row of RJ and MBRJ considering the ES1-P joint assembly. As anticipated, the introduction of the central bolt row improves the behavior under column loss by postponing the failure of the bolts.

5. Conclusions

This paper presents and discusses the results of a finite element parametric study devoted to investigate two aspects influencing the response of extended stiffened end-plate beam-to-column joints, namely the influence of yield strength of the end-plate material different from the design value and the presence of the central bolt row. On the basis of the obtained results, the following remarks can be drawn:

- The local and global response of joints with yield stress of the end-plate material different from the design value can change from the expected behavior in different way depending on the performance design level of the joint.
- The response of full strength joints under monotonic and cyclic loading is less affected by the variation of the end-plate material. Indeed, the design requirements guarantee large over-strength that ensures the formation of the plastic hinge into the beam, even in the cases with the weaker end-plate where some plastic deformations are observed.

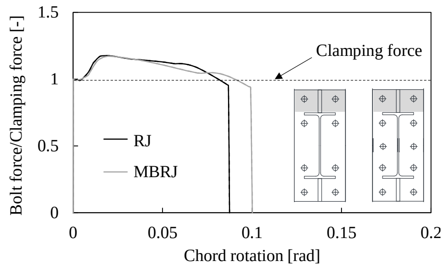

First bolt row

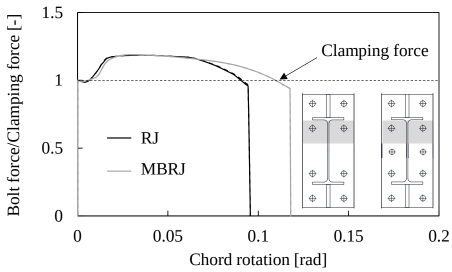

Second bolt row

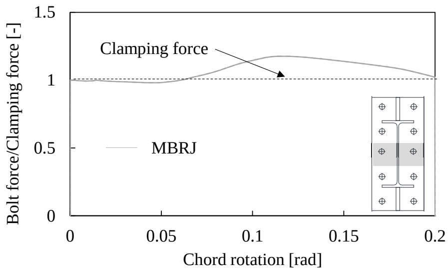

MBR bolt row

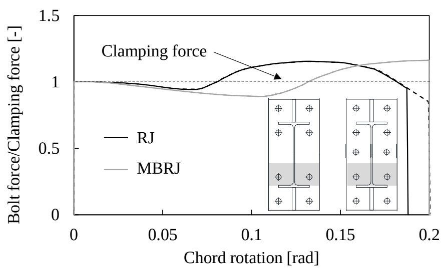

Third bolt row

Fig. 26 ES1-P bolts action: RJ vs MBRJ

Hence, the local response differs at the same overall response curve.

- The cyclic response of equal strength joints is highly influenced by the variation of the end-plate material. Indeed, the failure mode can move from the connection (i.e., partial strength joint) to the beam (i.e., full strength joint) with the increase of the end-plate yield strength. However, if the end-plate strength varies within the range ± 30% the design yield stress, the adopted capacity design criteria are effective to obtain plastic deformations in both beam and end-plate connection even though with different contribution.
- Yield stress lower than the design value can induce brittle failure into the welds of end-plate for partial strength joints due to the increase of the local demand in terms of plastic strain.
- The response of full strength joints under column loss is marginally influenced by the variation of the end-plate steel strength if the ratio $\Sigma F_{t,Rd}/N_{pl,Rd,\mathrm{Beam}}$ is close to 1. For ratios smaller than 0.90 the response of the full strength joints is deteriorated and it is affected by varying the end-plate steel strength.
- The resistance and the type of failure mode of both equal and partial strength joints under column loss is less influenced by the variation of the end-plate material strength. In both cases it is possible to observe a slight reduction of ductility when increasing the yield stress of the end-plate due to the premature failure of bolts.
- The central bolt row does not influence the moment-rotation response of the joints under both the cyclic and monotonic loading conditions. However, some slight differences can be observed comparing the dissipated energy of equal and partial strength joints. In those cases, the presence of the central bolt row reduces the gap opening of the connection and the pinching effects on the cyclic response curves. The reduction of natural frequency depends on the crack depth and crack location.
- The central bolt row has beneficial effects under column loss scenario. Indeed, increasing the axial strength and stiffness of the connection is effective to resist the catenary actions developed at large rotation demand.

Acknowledgments

The research activitypresented in this paper received funding from the European Union's Research Fund for Coal and Steel (RFCS) research program under the following grant agreements:

- *n*° RFSR-CT-2013-00021- European pre-QUALified steel JOINTS: EQUALJOINTS;
- *n*° 754048 — EQUALJOINTS-PLUS — RFCS-2016. The research described in this paper was financially supported by the Natural Science Foundation.

References

Abidelah, A., Bouchaïr, A. and Kerdal, D.E. (2012), "Experimental and analytical behavior of bolted end-plate connections with or without stiffeners", *J. Constr. Steel Res.*, **76**, 13-27.

ANSI/AISC 341-16 (2016), Seismic Provisions for Structural Steel Buildings; American Institute of Steel Construction, Chicago, IL, USA.

ANSI/AISC 358-16 (2016), Prequalified Connections for Special and Intermediate Steel Moment Frames for Seismic Applications; Chicago, IL, USA.

Augusto, H., Da Silva, L.S., Rebelo, C. and Castro, J.M. (2016), "Characterization of web panel components in double-extended bolted end-plate steel joints", *J. Constr. Steel Res.*, **116**, 271-293.

Augusto, H., Da Silva, L.S., Rebelo, C. and Castro, J.M. (2017), "Cyclic behaviour characterization of web panel components in bolted end-plate steel joints", *J. Constr. Steel Res.*, **133**, 310-333.

Brunesi, E., Nascimbene, R. and Rassati, G.A. (2014), "Response of partially-restrained bolted beam-to-column connections under cyclic loads", *J. Constr. Steel Res.*, **97**, 24-38.

Brunesi, E., Nascimbene, R. and Rassati, G.A. (2015), "Seismic response of MRFs with partially-restrained bolted beam-to-column connections through FE analyses", *J. Constr. Steel Res.*, **107**, 37-49.

Cassiano, D., D'Aniello, M., Rebelo, C., Landolfo, R. and Da Silva, L.S. (2016), "Influence of seismic design rules on the robustness of steel moment resisting frames", *Steel Compos. Struct., Int. J.*, **21**(3), 479-500.

Cassiano, D., D'Aniello, M. and Rebelo, C. (2017), "Parametric finite element analyses on flush end-plate joints under column removal", *J. Constr. Steel Res.*, **137**, 77-92.

Cassiano, D., D'Aniello, M. and Rebelo, C. (2018), "Seismic behaviour of gravity load designed flush end-plate joints", *Steel Compos. Struct., Int. J.*, **26**(5), 621-634.

CEN/TC 250/SC 3 N 2446, EN 1993-1-8 v.2.1 draft (2017-05-05), Eurocode 3 — Design of steel structures — Part 1-8: Design of joints, 10 May 2017.

D'Aniello, M., Cassiano, D. and Landolfo, R. (2016), "Monotonic and cyclic inelastic tensile response of European preloadable GR10.9 bolt assemblies", *J. Constr. Steel Res.*, **124**, 77-90.

D'Aniello, M., Cassiano, D. and Landolfo, R. (2017a), "Simplified criteria for finite element modelling of European preloadable bolts", *Steel Compos. Struct., Int. J.*, **24**(6), 643-658.

D'Aniello, M., Tartaglia, R., Costanzo, S. and Landolfo, R. (2017b), "Seismic design of extended stiffened end-plate joints in the framework of Eurocodes", *J. Constr. Steel Res.*, **128**, 512-527.

D'Aniello, M., Tartaglia, R., Costanzo, S., Campanella, G., Landolfo, R. and De Martino, A. (2018), "Experimental Tests on Extended Stiffened End-Plate Joints within Equal Joints Project", *Key Eng. Mater.*, **763**, 406-413. ISSN: 1662-9795

D'Antimo, M., Zimbru, M., D'Aniello, M., Demonceau, J-F., Jaspart, J-P. and Landolfo, R. (2018), "Preliminary Finite Element Analyses on Seismic Resistant FREE from DAMage Beam to Column Joints under Impact Loading", *Key Eng. Mater.*, **763**, 592-599, ISSN: 1662-9795.

Da Silva, L.S., Santiago, A. and Vila Real, P. (2002), "Post-limit stiffness and ductility of end-plate beam-to-column steel joints", *Comput. Struct.*, **80**(5-6), 515-531.

Dassault (2014), Abaqus 6.14 - Abaqus Analysis User's Manual; Dassault SystèmesSimulia Corp.

Dinu, F., Marginean, I. and Dubina, D. (2015), "Improving the structural robustness of multi-story steel-frame buildings", *Struct. Infrastruct. E*, **11**(8), 1028-1041.

Dinu, F., Marginean, I., Dubina, D. and Petran, I. (2016), "Experimental testing and numerical analysis of 3D steel frame system under column loss", *Eng. Struct.*, **113**, 59-70.

Dutta, A., Dhar, S. and Acharyya, S.K. (2010), "Material characterization of SS 316 in low cycle fatigue loading", *J. Mater. Sci.*, **45**(7), 1782-1789.

El-Tawil, S., Vidarsson, E., Mikesell, T. and Kunnath, S.K. (1999), "Inelastic behaviour and design of steel panel zones", *J. Struct. Eng.*, **125**(2), 183-193.

EN 10034 (1993), Structural Steel I and H Sections: Tolerances on Shape and Dimensions; European Committee for Standardization, Brussels, Belgium.

EN 1993-1-1 (2005), Eurocode 3: Design of steel structures. Part 1-1: General rules and rules for buildings; European Committee for Standardization, Brussels, Belgium.

EN 1993 1-8 (2005), Eurocode 3: Design of Steel Structures. Part 1-8: Design of Joints; European Committee for Standardization, Brussels, Belgium.

EN 1998-1 (2005), Design of Structures for Earthquake Resistance. Part 1: General Rules, Seismic Actions and Rules for Buildings; European Committee for Standardization, Brussels, Belgium.

EN ISO 2560 (2009), Welding consumables - Covered electrodes for manual metal arc welding of non-alloy and fine grain steels – Classification; European Committee for Standardization, Brussels, Belgium.

Faella, C., Piluso, V. and Rizzano, G. (2000), *Structural Steel Semi-Rigid Connections – Theory, Design and Software*, CRC Press LLC, Boca Raton, FL, USA.

Girao Coelho, A.M., Da Silva, L.S. and Bijlaard, F.S.K. (2004), "Experimental assessment of the ductility of extended end plate connections", *Eng. Struct.*, **26**(9), 1185-1206.

Guo, B., Gu, Q. and Liu, F. (2006), "Experimental Behavior of Stiffened and Unstiffened End-Plate Connections under Cyclic Loading", *J. Struct. Eng.*, **132**(9), 1352-1357.

Huvelle, C., Hoang, V., Jaspart, J.P. and Demonceau, J.F. (2015), "Complete analytical procedure to assess the response of a frame submitted to a column loss", *Eng. Struct.*, **86**, 33-42.

Iannone, F., Latour, M., Piluso, V. and Rizzano, G. (2010), "Experimental analysis of bolted steel beam-to-column connections: component identification", *J. Earth. Eng.*, **15**(2), 212-244.

Izzudin, B., Vlassis, A., Elghazouli, A. and Nethercot, D. (2008), "Progressive collapse of multi-storey buildings due to sudden column loss - Part I: Simplified assessment framework", *Eng. Struct.*, **30**(5), 1308-1318.

Landolfo, R., D'Aniello, M., Costanzo, S., Tartaglia, R., Stratan, A., Dubina, D., Vulcu, C., Maris, C., Zub, C., Da Silva, L.S., Rebelo, C., Augusto, H., Shahbazian, A., Gentili, F., Jaspart, J.P., Demonceau, J.F., Hoang, L.V., Elghazouli, A., Tsitos, A., Vassart, O., Nunez, E.M., Dehan, V. and Hamreza, C. (2017), "European pre-QUALified steel JOINTS: EQUALJOINTS" Final report, European Commission, Research Programme of the Research Fund for Coal and Steel - TG S8.

Latour, M. and Rizzano, G. (2013), "Full strength design of column base connections accounting for random material variability", *Eng. Struct.*, **48**, 458-471.

Latour, M., Piluso, V. and Rizzano, G. (2011), "Cyclic modeling of bolted beam-to-column connections: Component approach", *J. Earthq. Eng.*, **15**(4), 537-563.

Latour, M., Piluso, V. and Rizzano, G. (2014), "Experimental Analysis on the Cyclic Response of Beam to Column Joints: State-of-the-Art at Salerno University", *Open Constr. Build. Technol. J.*, **8**, 227-247.

Latour, M., Piluso, V. and Rizzano, G. (2018), "Experimental analysis of beam-to-column joints equipped with sprayed aluminium friction dampers", *J. Const. Steel Res.*, **146**, 33-48.

Leon, R.T. (1995), "Seismic Performance of Bolted and Riveted Connections", Background Reports; Metallurgy, Fracture Mechanics, Welding, Moment Connections and Frame System Behavior, Report No SAC-95-09, FEMA-288 / March 1997, Federal Emergency Management Agency, Washington, DC, USA.

Maggi, Y.I., Gonçalves, R.M., Leon, R.T. and Ribeiro, L.F.L. (2005), "Parametric analysis of steel bolted end plate connections using finite element modelling", *J. Constr. Steel Res.*, **61**(5), 689-708.

Murray, T.M. (1990), AISC Design Guide 4, Extended End-Plate Moment Connections, AISC (American Institute of Steel Construction), Chicago, IL, USA.

Murray, T.M. and Sumner, E.A. (2004), AISC Design Guide 4, Extended End-Plate Moment Connections—Seismic and Wind Applications, (2nd Edition), AISC (American Institute of Steel Construction), Chicago, IL USA.

OPTIFIN: Optimisation of finishing processes for eliminating rectification of plate and section products - RFSR-CT-2007-00014.

OPUS: Optimising the seismic performance of steel and steel-concrete structures by standardising material quality control-RFSR-CT-2007-00039.

Pavlovic, M., Heistermann, C., Veljkovic, M., Pak, D., Feldmann, M., Rebelo, C. and Da Silva, L.S. (2015), "Connections in towers for wind converters, part I: Evaluation of down-scaled experiments", *J. Const. Steel Res.*, **115**, 445-457.

Piluso, V. and Rizzano, G. (2007), "Random material variability effects on full-strength end-plate beam-to-column joints", *J. Constr. Steel Res.*, **63**(5), 658-666.

Piluso, V., Rizzano, G. and Tolone, I. (2012), "Moment resistance statistical distribution of beam-to-column composite joints", *J. Constr. Steel Res.*, **78**, 183-191.

Sadek, F., Main, J., Lew, H. and El-Tawil, S. (2013), "Performance of steel moment connections under a column removal scenario. II: Analysis", *J. Struct. Eng.*, **139**(1), 108-119.

SAFEBRICTILE: Standardization of Safety Assessment Procedures across Brittle to Ductile Failure Modes - RFSR-CT-2013-00023.

Shi, Y., Shi, G. and Wang, Y. (2007a), "Behaviour of end-plate moment connections under earthquake loading", *Eng. Struct.*, **29**(5), 703-716.

Shi, Y., Shi, G. and Wang, Y. (2007b), "Experimental and theoretical analysis of the moment-rotation behaviour of stiffened extended end-plate connections", *J. Constr. Steel Res.*, **63**(9), 1279-1293.

Sumner, E.A. and Murray, T.M. (2000), "Performance of Extended Moment End-Plate Connections Subject to Seismic Loading", *U.S.–Japan Workshop on Seismic Fracture Issues in Steel Structures*, San Francisco, CA, USA, February-March.

Sumner, E.A. and Murray, T.M. (2002), "Behavior of extended end-plate moment connections subject to cyclic loading", *J. Struct. Eng.*, **128**(4), 501-508.

Tartaglia, R. and D'Aniello, M. (2017), "Nonlinear performance of extended stiffened end plate bolted beam-to-column joints subjected to column removal", *Open Civ. Eng. J.*, **11**(Suppl-1, M6), 369-383.

Tartaglia, R., D'Aniello, M., Rassati, G.A., Swanson, J.A. and Landolfo, R. (2018a), "Full strength extended stiffened end-plate joints: AISC vs recent European design criteria", *Eng. Struct.*, **159**, 155-171.

Tartaglia, R., D'Aniello, M., Rassati, G.A., Swanson, J.A. and Landolfo, R. (2018b), "Influence of Composite Slab on the Nonlinear Response of Extended End-Plate Beam-to-Column Joints", *Key Eng. Mater.*, **763**, 818-825. ISSN: 1662-9795.

Yang, B. and Tan, K. (2013), "Experimental tests of different types of bolted steel beam-column joints under a central-column removal scenario", *Eng*. *Struct*., **54**, 112-130.

CC